A Non-Obese Hyperglycemic Mouse Model that Develops after Birth with Low Birthweight

日本大学大学院医学研究科博士課程
内科系小児科学専攻

片山 大地
修了年 2023 年
指導教員 長野 伸彦

biomedicines

MDPI

A Non-Obese Hyperglycemic Mouse Model that Develops after Birth with Low Birthweight

Daichi Katayama [†], Nobuhiko Nagano [†], Shoichi Shimizu, Kimitaka Nakazaki, Kengo Matsuda, Wataru Tokunaga, Kazumasa Fuwa, Ryoji Aoki and Ichiro Morioka *

Department of Pediatrics and Child Health, Nihon University School of Medicine, Tokyo 173-8610, Japan; katayama.daichi@nihon-u.ac.jp (D.K.); nagano.nobuhiko@nihon-u.ac.jp (N.N.); shimizu.shoichi@nihon-u.ac.jp (S.S.); nakazaki.kimitaka@nihon-u.ac.jp (K.N.); matsuda.kengo@nihon-u.ac.jp (K.M.); tokunaga.wataru@nihon-u.ac.jp (W.T.); fuwa.kazumasa@nihon-u.ac.jp (K.F.); aoki.ryoji@nihon-u.ac.jp (R.A.)
* Correspondence: morioka.ichiro@nihon-u.ac.jp; Tel.: +81-3-3972-8111
† These authors contributed equally to this work.

Abstract: The number of low birthweight (LBW) infants weighing below 2500 g has not decreased in Japan. This study aimed to develop an adult non-obese hyperglycemic mouse model born with LBW to study the pathogenesis. At 16.5 days of gestation, transient intrauterine ischemia (blocked blood flow in both uterine arteries for 15 min) was performed in a subgroup of pregnant mice (group I). Non-occluded dams were used as sham controls (group C). After birth, female pups in each group were weaned at 4 weeks of age and reared on the normal diet until 8 weeks of age ($n = 7$). Fasting blood glucose levels, serum immunoreactive insulin (IRI), and body composition were then measured. Metabolite analyses was performed on the liver tissues. Birthweight was significantly lower in group I compared with group C. Pups from group I remained underweight with low fat-free mass and showed hyperglycemia with high serum IRI and homeostasis model assessment of insulin resistance levels, indicating insulin resistance. Metabolite analyses showed significantly reduced adenosine triphosphate and nicotinamide adenine dinucleotide production and increased lactic acid in group I. The pathogenesis of our non-obese hyperglycemic mouse model may be due to increased myogenic insulin resistance based on mitochondrial dysfunction and reduced lean body mass.

Keywords: body composition; developmental origins of health and disease; homeostasis model assessment of insulin resistance; immunoreactive insulin; metabolite analyses; myogenic insulin resistance

1. Introduction

Fetuses exposed to undernutrition by lean pregnant women with nutritional restrictions during pregnancy lose weight and acquire insulin resistance and a frugal constitution that easily accumulates energy-efficient fat through the adaptation of metabolic and endocrine mechanisms to the undernutrition environment in utero [1,2]. Low birthweight (LBW) infants are more likely to develop metabolic syndrome and lifestyle-related diseases such as type 2 diabetes mellitus, hyperlipidemia, and hypertension in adulthood (developmental origins of health and disease [DOHaD] theory) [3].

The total number of births in Japan is decreasing, yet the trend of LBW infants weighing under 2500 g has not decreased [4]. The percentage of LBW infants in the total annual number of births is 9.49%, which is higher than that of other countries (8.02% in the United States, 6.95% in the United Kingdom, 6.65% in Germany, 4.95% in China, and 8.38% in Brazil) [5]. Therefore, it is very important to reduce adulthood health problems in LBW infants for medical, economic, and social reasons.

It has been reported that a Japanese patient born with LBW developed type 2 diabetes mellitus without being markedly obese at a young age [6]. Some diabetic patients in Japan

are non-obese and have a normal body mass index (BMI, 24.9 kg/m^2 or less) [7]. Indeed, Japanese type 2 diabetes patients were less obese than those in Western countries [8]. Approximately 15% of Japanese children with type 2 diabetes are non-obese, which is a higher rate than that in other countries [9]. It is still unclear why there are so many non-obese type 2 diabetes patients in Japan, and the scientific reasons are under research.

Animal models wherein obese type 2 diabetes develops after birth with LBW by a eutrophic (high fat) diet already exist [10]. However, there is no animal model wherein non-obese hyperglycemia develops after birth at LBW. The cause of non-obese type 2 diabetes is thought to be insulin resistance due to fat accumulation in the liver and skeletal muscle as visceral or ectopic fat [11]. In humans, the relationship between the development rate of type 2 diabetes and birth weight shows a U-shape [12], suggesting that future visceral fat accumulation occurs regardless of whether birthweight is high or low. However, the mechanisms of insulin resistance and details of body composition are unclear in non-obese type 2 diabetes that develops after birth at LBW.

The aims of this study were to develop a mouse model with non-obese hyperglycemia that develops after birth at LBW and to clarify the pathogenetic mechanism of non-obese hyperglycemia in our mouse model.

2. Materials and Methods

2.1. Study Design, Protocol, and Animal Model

This study was carried out in accordance with the ARRIVE guidelines, and the protocols were approved by the Nihon University Institutional Animal Care and Use Committee (protocol nos. AP18MED033-1 [5 July 2019] and AP20MED003-1 [3 April 2020]). ICR mice strains at 12 days of gestation were obtained from Sankyo Labo Service Corporation Inc., Tokyo, Japan. All mice were fed a normal solid diet (moisture: 7.9%, crude fat: 5.1%, crude protein: 23.1%, crude ash: 5.8%, crude fiber: 2.8%, and soluble solids: 55.3% (Oriental Yeast Co., Ltd., Tokyo, Japan) and had access to water ad libitum.

The lower abdomen was incised under isoflurane inhalation anesthesia (induction 5%, maintenance 2%) at 16.5 days of gestation. In the intrauterine ischemia (group I), maternal mice were pre-warmed at 37.5 °C on a hot plate, the uterine artery was exposed and blood flow to the artery was blocked by a clip for 15 min to lead to fetus hypoxia and undernutrition (Figure 1a,b) [13]. The uterine artery was then unclipped, the were fetuses returned into the abdomen of the mother mice, and the abdomen was sutured. The controls (group C) only underwent a lower abdominal incision under similar anesthesia (sham control). Newborn pups were reared under the care of their mothers; female pups from the two groups were weaned at 4 weeks of age after birth and reared on a normal diet until 8 weeks of age (Figure 1c).

At birth and thereafter, the pups were weighed twice a week until 8 weeks of age. The body weight gain plateaued at approximately 8 weeks of age. Eight-week-old mice represent human adulthood [14]. At 8 weeks of age, body composition was measured, blood was drawn from the heart, and the liver was removed after 12 h of fasting (Figure 1c,d). Fasting blood glucose levels, serum immunoreactive insulin (IRI), body composition, and serum lipoprotein levels were measured at 8 weeks of age. Metabolite analyses were performed on liver tissues at 8 weeks of age. Results were compared between group I and C (*n* = 7 for each group).

2.2. Glucose Metabolism Markers

Blood glucose levels after 12 h of fasting were measured using a Stat Strip XP2 (Nipro Corp., Osaka, Japan). Blood was then centrifuged at 3000 rpm for 5 min at room temperature and the serum was stored at −20 °C. Serum IRI levels were measured using a mouse/rat total insulin (high sensitivity) assay kit (Immuno-Biological Laboratories Co., Ltd., Fujioka, Gunma, Japan). Homeostasis model assessment of insulin resistance (HOMA-R) was calculated using the human formula:

$$\text{HOMA-R} = \text{fasting blood glucose (mg/dL)} \times \text{IRI (μIU/mL)}/405$$
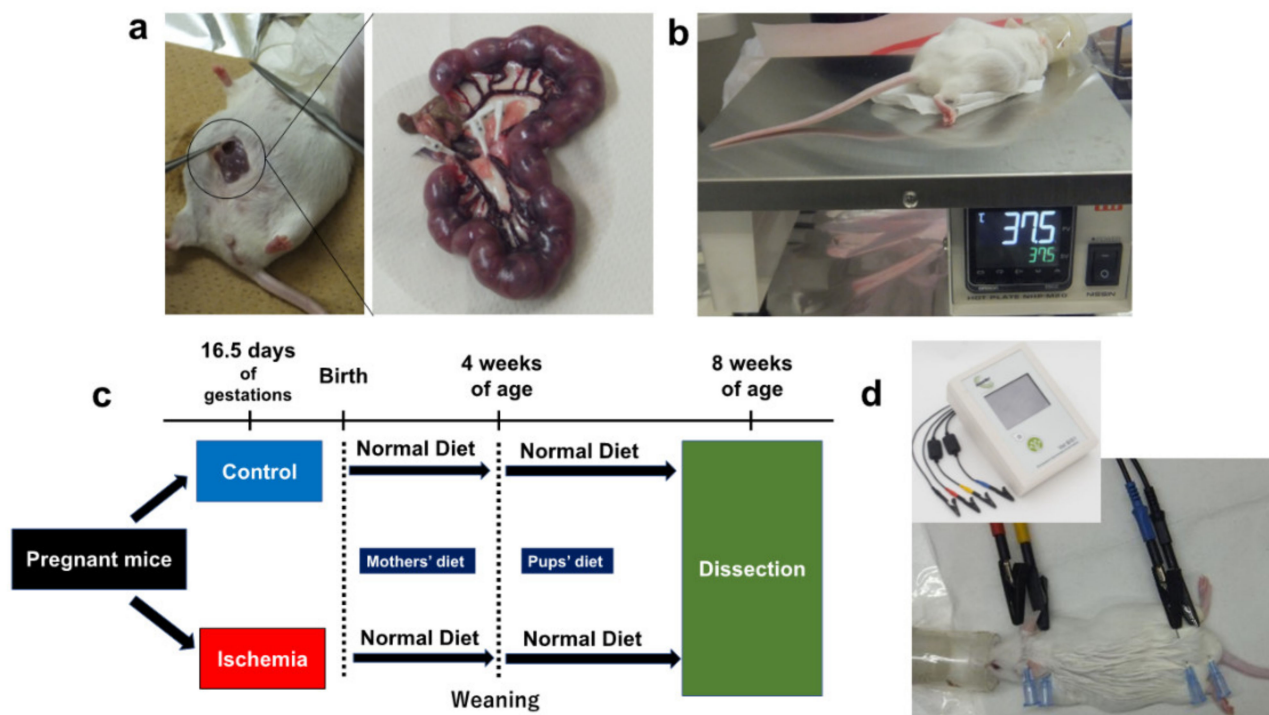
since there is no formula for mice [15].

Figure 1. Experimental procedures. (**a**) Uterine artery ligation in pregnant mice (ischemia for 15 min). (**b**) Body temperature control on a hot plate (37.5 °C). (**c**) Study flow of this study. (**d**) Body composition measurements using ImpediVET^{TM} (Bioresearch center, Co., Ltd., Nagoya, Japan).

2.3. Body Composition Analyses

Body composition was measured using the bioelectrical impedance analysis method using a body composition analyzer for laboratory animals (ImpediVET^{TM}, Bioresearch center, Co., Ltd., Nagoya, Japan) (Figure 1d) [15]. Bioelectrical impedance analysis is used to estimate body composition (such as body fat percentage) by measuring the electrical resistance (bioimpedance) of biological tissues. Adipose tissue conducts almost no electricity, while muscle and other tissues that contain many electrolytes easily conduct electricity. The ratio of fat to other tissues can be estimated by measuring electrical resistance [16]. Fat mass percentage and fat-free mass percentage were measured. Fat mass (g) (1) or fat-free mass (g) (2) were calculated using the following formula:

(1) Fat mass (g) = eight-week-old body weight (g) × fat mass percentage/100
(2) Fat-free mass (g) = eight-week-old body weight (g) × fat-free mass percentage/100

2.4. Serum Lipoprotein Levels

Cholesterol and triglyceride profiles in serum lipoproteins were analyzed using a previously described gel-permeation high-performance liquid chromatography method (LipoSEARCH®; Skylight Biotech, Akita, Japan) [17–19]. Cholesterol and triglyceride levels of total- and major classes of lipoproteins (high density lipoprotein, HDL; low density lipoprotein, LDL; very low-density lipoprotein, VLDL) were defined using component peak analyses based on lipoprotein particle sizes using the Gaussian curve fitting technique [18].

2.5. Metabolite Analyses in Liver

Metabolites were extracted using the following methods: approximately 50 mg of frozen liver tissue from female mice (8 weeks of age, *n* = 3 each group) was placed in a homogenization tube along with zirconia beads (5 mm φ and 3 mm φ). Next, 1500 μL of 50% acetonitrile/Milli-Q water containing internal standards (H3304-1002, Human Metabolome Technologies, Inc. (HMT), Tsuruoka, Yamagata, Japan) was added, followed by two cycles

of tissue homogenization using a bead shaker at 1500 rpm for 120 s at 4 °C each (Shake Master NEO, Bio Medical Science, Tokyo, Japan). The homogenate was centrifuged at $2300 \times g$ for 5 min at 4 °C. The upper aqueous layer (400 μL) was centrifugally filtered at $9100 \times g$ for 120 min at 4 °C using a Millipore 5-kDa cutoff filter (Human Metabolome Technologies, Inc.) to remove macromolecules. Under vacuum, the filtrate was evaporated to dryness and redissolved in 50 μL of Milli-Q water for the metabolome analysis.

Metabolome analyses were conducted using capillary electrophoresis time-of-flight mass spectrometry, as previously described [20,21]. Briefly, capillary electrophoresis time-of-flight mass spectrometry analysis was performed using an Agilent CE capillary electrophoresis system (Agilent Technologies, Inc., Santa Clara, CA, USA). The spectrometer was scanned at 50–1000 m/z and peaks were extracted by integration software (Keio University, Tsuruoka, Yamagata, Japan) to obtain the following data; m/z, migration time, and peak area [22]. The peaks were determined according to the metabolite database based on their m/z values and migration times. Peak areas were normalized using internal standards and sample volume, then relative levels of the metabolites were obtained.

Principal component analysis and hierarchical cluster analysis were performed, as previously described [23]. Detected metabolites were plotted on metabolic pathway maps, as previously described [24].

2.6. Statistical Analyses

Data are expressed as the mean ± standard error of the mean. Comparisons between the two groups were performed with the Mann-Whitney U test or Welch's *t* test as appropriate using JMP ver. 14 (SAS Institute, Cary, NC, USA). A *p* value < 0.05 was considered a significant difference.

3. Results

3.1. Birth Weight and Changes in Body Weight Gain

Birthweight was significantly lower in group I (1.5 g) than that in group C (1.8 g) ($p = 0.01$) (Figure 2a). The mean body weights of groups I and C at 1, 2, 3, 4, 5, 6, 7, and 8 weeks of age were: 4.7 and 7.2 g, $p < 0.01$; 7.3 and 9.7 g, $p < 0.01$; 14.0 and 15.5 g, $p = 0.03$; 22.1 and 26.1 g, $p < 0.01$; 30.5 and 34.1 g, $p < 0.01$; 33.2 and 36.3 g, $p = 0.02$; 33.9 and 37.9 g, $p < 0.05$; and 35.5 and 40.2 g, $p = 0.01$, respectively. Group I had a LBW and was consistently underweight thereafter, even at 8 weeks of age (Figure 2b).

3.2. Glucose Metabolism Markers

The mean fasting blood glucose level at 8 weeks of age was significantly higher in group I compared with group C (196.9 and 75.0 mg/dL, respectively) ($p < 0.01$). The mean levels of IRI and HOMA-R were significantly higher in group I (3.9 μIU/mL and 1.9, respectively) compared with group C (1.4 μIU/mL and 0.3, respectively) ($p = 0.03$, $p < 0.01$, respectively; Figure 2c–e).

3.3. Body Composition

There was no significant difference between the mean fat mass of group I and group C (16.6 and 17.7 g, respectively) ($p = 0.95$, Figure 3a). Meanwhile, the mean fat-free mass was significantly lower in group I than that of group C (19.1 and 22.6 g, respectively) ($p = 0.01$, Figure 3b).

3.4. Serum Lipoprotein Levels

Mean total cholesterol, LDL cholesterol, VLDL cholesterol, and HDL cholesterol levels were 104.4 mg/dL, 15.5 mg/dL, 10.7 mg/dL, and 77.6 mg/dL, respectively in group I and 99.3 mg/dL, 16.5 mg/dL, 8.2 mg/dL, and 74.3 mg/dL, respectively in group C, with no significant differences between the two groups (Figure 3c–f). Total triglyceride level was significantly higher in Group I (88.1 mg/dL) than that of group C (37.3 mg/dL) ($p < 0.05$; Figure 3g).
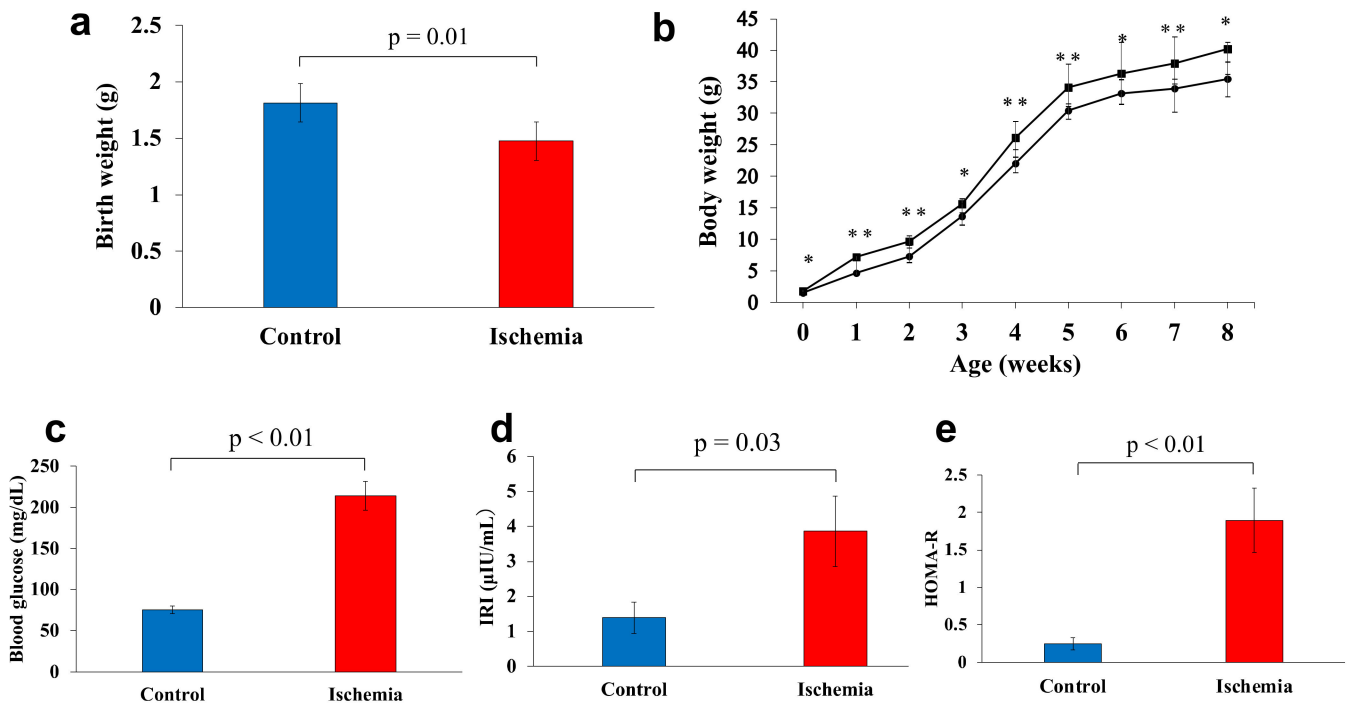
Figure 2. Body weight and glucose metabolism markers. (**a**) Birthweight was measured on the first day after birth. (**b**) Changes in weight gain from birth to 8 weeks of age (●: Ischemia, ■: Control). (**c**) Fasting blood glucose levels. (**d**) Serum immunoreactive insulin levels. (**e**) Homeostasis model assessment of insulin resistance levels. Data are shown as the mean ± standard error of the mean ($n = 7$ per group). * $p < 0.05$, ** $p < 0.01$.
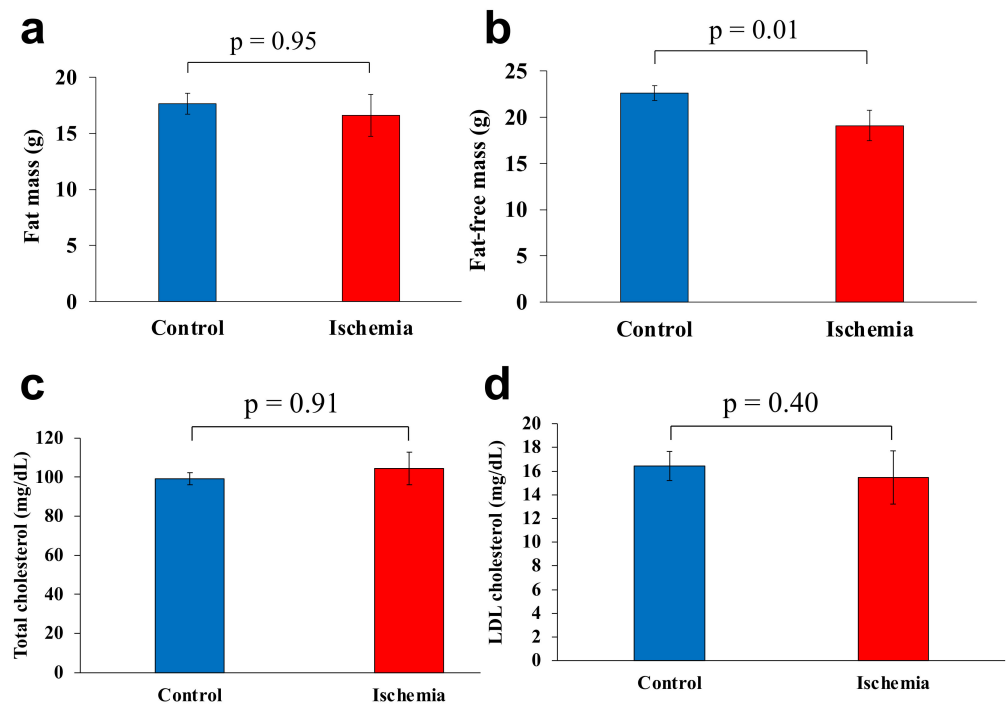
Figure 3. *Cont.*
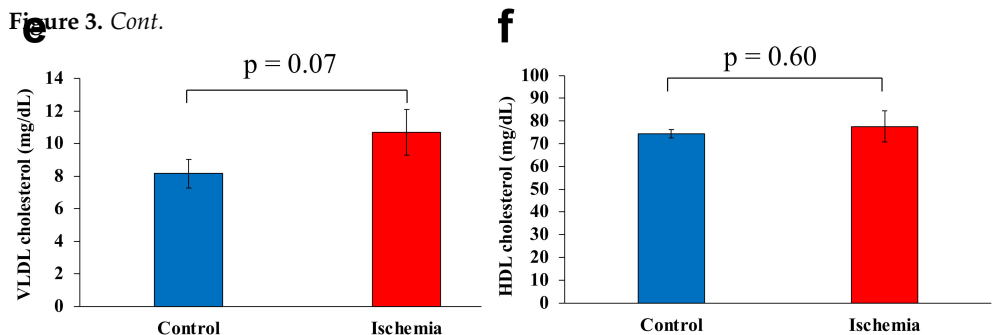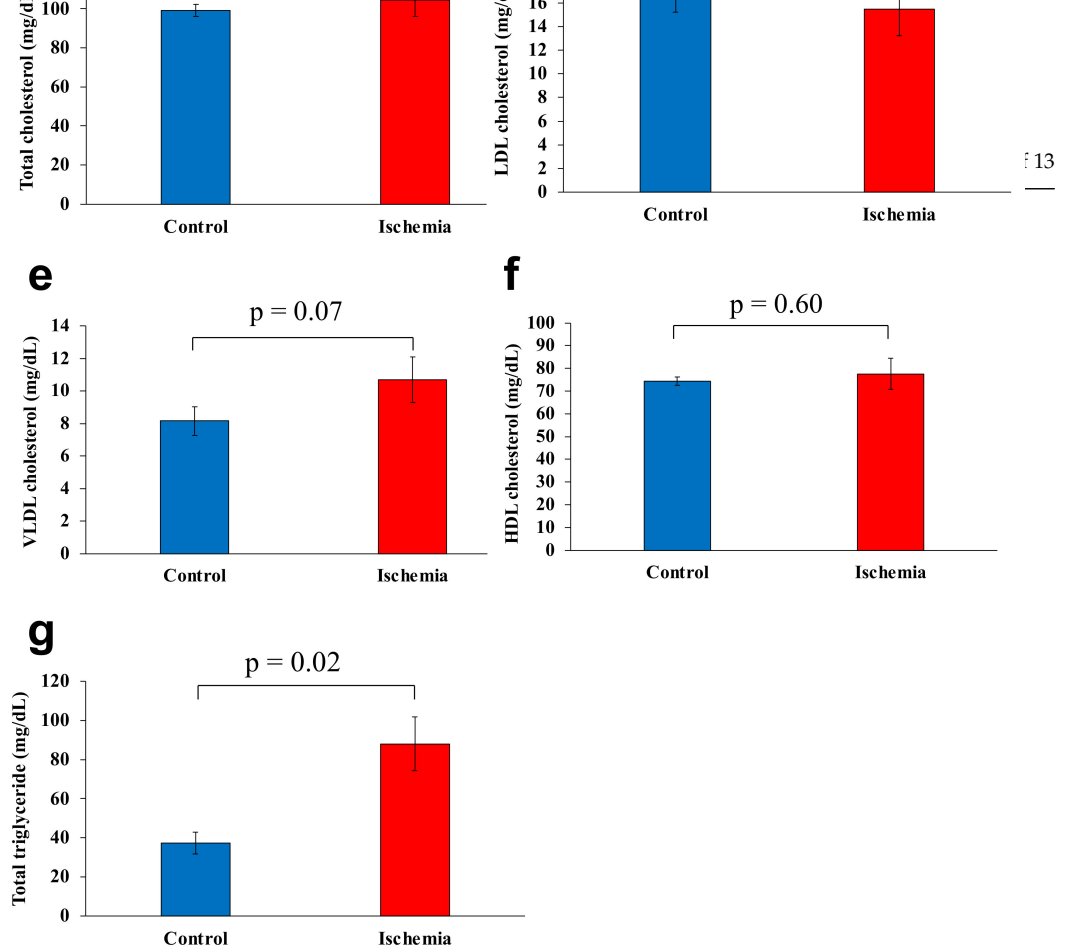
Figure 3. Body composition and serum lipoprotein levels. (**a**) Fat mass. (**b**) Fat-free mass. (**c**) Total cholesterol. (**d**) LDL cholesterol. (**e**) VLDL cholesterol. (**f**) HDL cholesterol. (**g**) Total triglyceride. Data are shown as the mean ± standard error of the mean (*n* = 7 per group). HDL, high-density lipoprotein; LDL, low-density lipoprotein; VLDL, very-low-density lipoprotein.

3.5. Liver Metabolite Analyses

A clear difference was found between group I and group C in the principal component analysis and the heat map display of the hierarchical cluster analysis (*n* = 3 for each group, Figure 4a,b; Supplementary Tables S1 and S2).
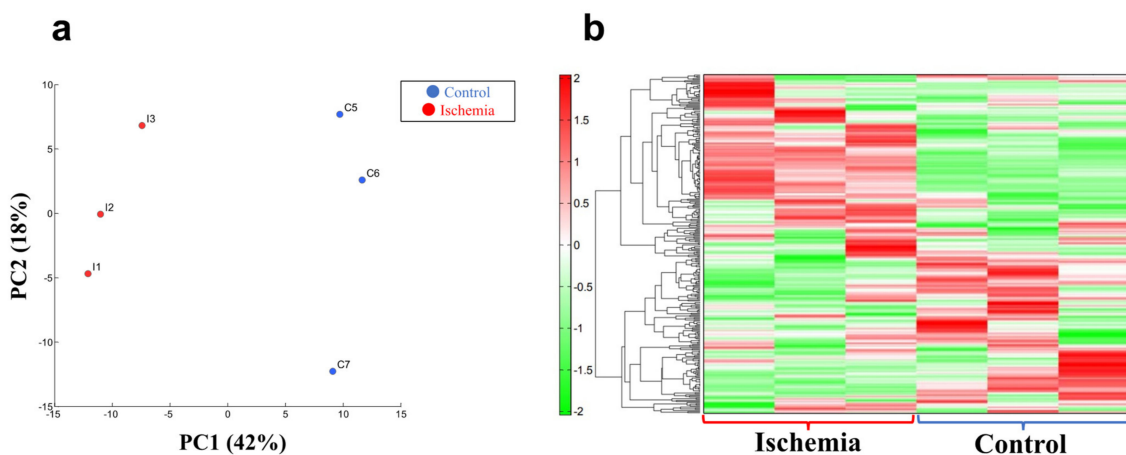
Figure 4. Metabolite analyses in liver tissue. (**a**) Principal component (PC) analysis. (**b**) Heat map display of the hierarchical cluster analysis. *n* = 3 per group.

Comparative analysis of the tricarboxylic acid (TCA) cycle, respiratory chain, and glycolytic pathway between group I and C are shown in Figure 5a,b, and Supplementary Table S3. Malic acid, fumaric acid, succinic acid, and citric acid were higher in group I than group C ($p < 0.001$, $p < 0.001$, $p = 0.170$, and $p = 0.118$, respectively; Figure 5c). Respiratory chain analyses showed that nicotinamide adenine dinucleotide (NAD^+) and adenosine triphosphate (ATP) were significantly lower in group I than that of group C ($p = 0.010$ and $p = 0.031$, respectively). Meanwhile, lactic acid in the glycolytic pathway was significantly

higher in group I than that in group C ($p = 0.002$). Representative oxidative stress markers 3-indoxylsulfuric acid, cysteine, and S-adenosylmethionine were significantly higher in group I than that in group C ($p < 0.001$, $p < 0.05$, and $p < 0.01$, respectively; Table 1).
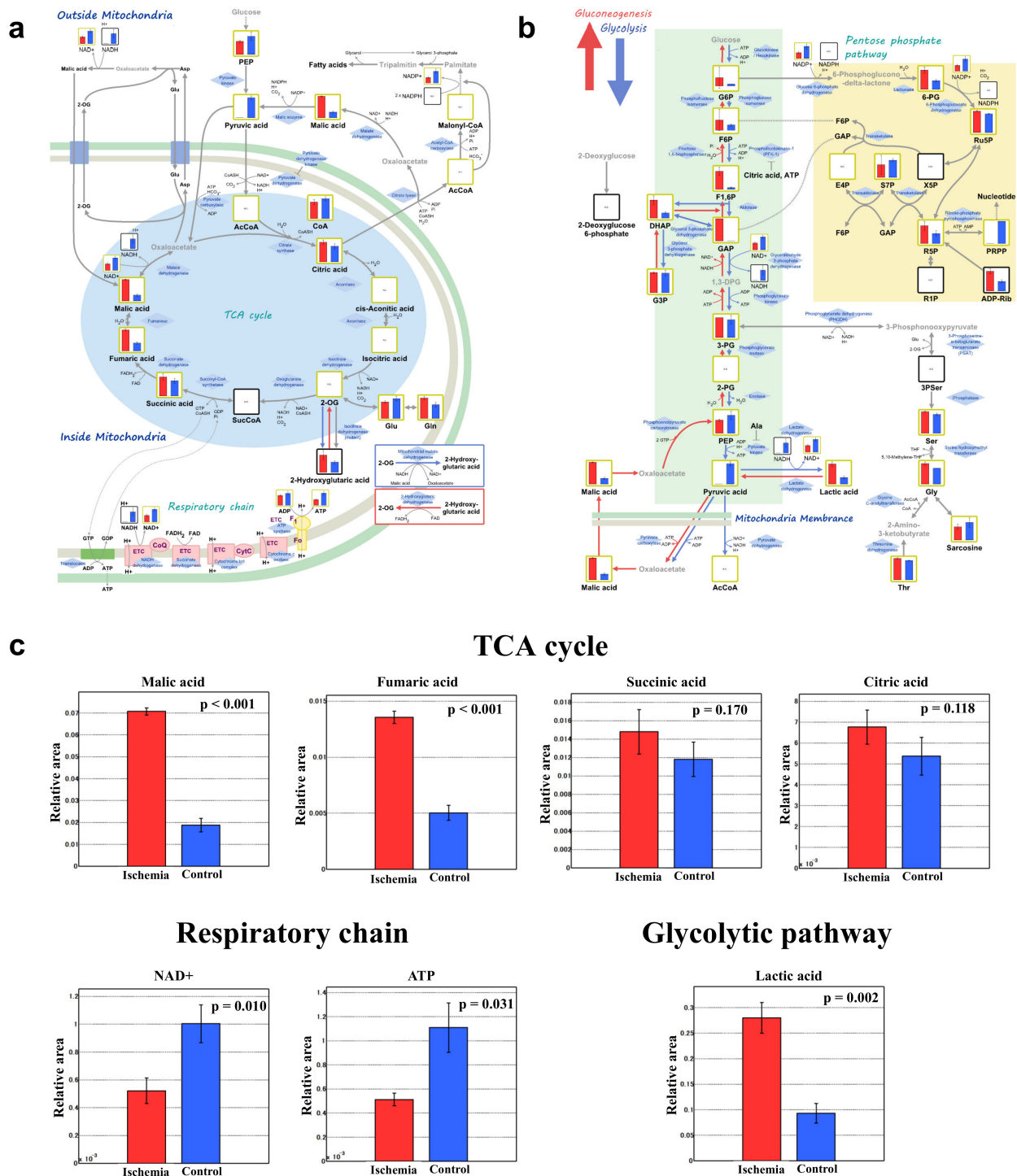
Figure 5. Comprehensive comparative analysis between the ischemia and control groups for the TCA cycle, respiratory chain, and glycolytic pathway. (**a**) TCA cycle and respiratory chain. (**b**) Glycolytic pathway. (**c**) Important metabolites. Red and blue bars show group I and C, respectively. ATP, adenosine triphosphate; NAD$^+$; nicotinamide adenine dinucleotide; TCA, tricarboxylic acid; $n = 3$ per group.

Table 1. Oxidative stress markers.

Compound Name	Compound Name	Comparative Analysis	
		Group I vs. C	
		Ratio [†]	*p*-Value [‖]
Oxidative stress	3-indoxylsulfuric acid	2.0	<0.001
	Cys	3.0	0.011
	S-adenosylmethionine	1.7	0.003
	Ergothioneine	0.7	0.061
	N,*N*-dimethylglycine	0.9	0.683

[†] The ratio of the detected mean values between the two groups. [‖] Welch's *t*-test.

4. Discussion

In clinical practice, patients born with LBW can develop type 2 diabetes without significant postnatal obesity; however, animal models have not yet been developed. In this study, we confirmed that our mouse model using intrauterine ischemia by transiently blocking blood flow of uterine arteries in pregnant mice yields non-obese hyperglycemia in young adulthood after birth with LBW. Total cholesterol, LDL cholesterol, VLDL cholesterol, and HDL cholesterol levels were not significantly different from the controls. Reduced lean body mass and mitochondrial dysfunction contributed to the increased myogenic insulin resistance of non-obese hyperglycemia (Figure 6).
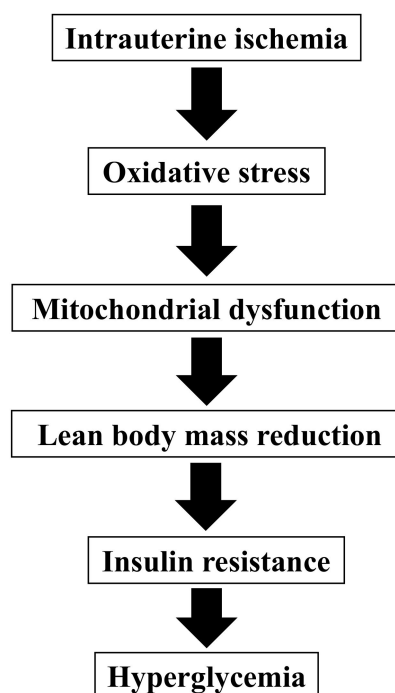
Figure 6. A theory for the pathogenesis of non-obese hyperglycemia after birth with low birthweight in our model.

4.1. Mice Model Born with LBW

Intrauterine malnutrition, such as ligation of bilateral uterine arteries in pregnant rats or food restriction of pregnant animals, can cause fetal growth restriction [25–28]. There are animal models that develop hyperglycemia with adulthood obesity [10] and that remain underweight in adulthood but do not develop hyperglycemia [29]. However, this is the first animal model that develops hyperglycemia after birth with LBW without developing adulthood obesity on a normal diet. Further studies are needed to investigate if

the pathogenesis of our mouse model is related to that of human non-obese type 2 diabetic patients.

4.2. Myogenic Insulin Resistance

Group I had significantly lower fat-free mass than that of group C, although there was no difference in fat mass between the groups. This may be due to decreased muscle mass in group I since this group was not obese. Patients born with LBW tend to have low muscle mass in adulthood [30] and their basal metabolism is low [31] which leads to visceral fat accumulation, decreased adiponectin secretion, and insulin resistance [32]. Our animal model showed myogenic insulin resistance due to reduced muscle mass which is considered one of the causes of non-obese diabetes.

4.3. Mitochondrial Dysfunction

Mitochondria are the site of energy production such as ATP; therefore, mitochondrial dysfunction decreases ATP production. Lactic acid increases since ATP is produced through anaerobic glycolysis [33]. NAD^+ is one of the cofactors for energy production in mitochondria and is also reduced by mitochondrial dysfunction [34]. In this study, group I liver metabolite analyses showed decreased mitochondrial function through decreased ATP production, increased lactic acid, and decreased NAD^+. In addition, 3-indoxylsulfuric acid (an oxidative stress molecule) was significantly higher in group I compared with group C. Ischemia and reperfusion produce oxidative stress, such as reactive oxygen species, resulting in decreased mitochondrial function [35–38]; this suggests that the intrauterine ischemia in the present model caused mitochondrial dysfunction by the same mechanism (Figure 7).
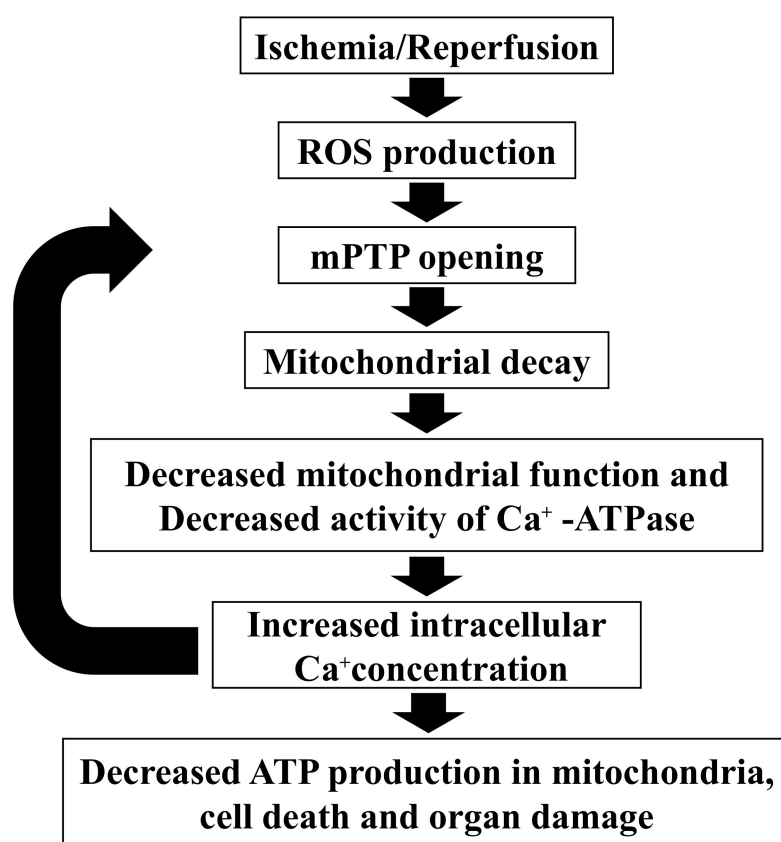
Figure 7. Mitochondria dysfunction by ischemia and reperfusion. ATP, adenosine triphosphate; mPTP, mitochondrial permeability transition pore; ROS, reactive oxygen species.

Diabetes development is strongly associated with mitochondrial dysfunction in skeletal muscle and liver; therefore, mitochondrial dysfunction can cause insulin resistance [39]. The clinical features of mitochondrial diabetes include short stature and non-obesity [40]. The development of mitochondrial diabetes is at a relatively young age (in the 30s), and the maternal inheritance of diabetes mellitus is 59%; therefore, not all cases are maternally inherited. Mitochondrial diabetes varies from insulin deficiency to insulin resistance. It is thought that autoimmune mechanisms are less likely to be involved. Other reports demonstrated a link between insulin resistance and mitochondrial dysfunction in the elderly [41] and mitochondrial dysfunction in a close relative of a diabetic patient [41]. Furthermore, type 2 diabetic patients have decreased expression of mitochondrial respiratory chain complexes or mitochondrial metabolism-related genes compared with healthy controls [42,43] while continuous physical activity improves insulin resistance and mitochondrial dysfunction in type 2 diabetic patients and obese individuals [44]. In addition, decreased mitochondrial DNA in peripheral blood cells correlates with insulin resistance [45] suggesting that quantitative or qualitative mitochondrial decline may be involved in the development of non-obese type 2 diabetes. Mitochondrial dysfunction causes muscle atrophy [46] and may be associated with insulin resistance due to reduced muscle mass which is the cause of non-obese type 2 diabetes.

4.4. Other Pathogeneses

As other pathogeneses, increased insulin clearance [47], decreased pancreatic β-cell function [48], and enlarged fat cells [49] have been reported in the cause of non-obese type 2 diabetes. It is necessary to study if these causes exist in this model using biochemical, genetic, and histopathological analyses.

4.5. Limitations

There were several limitations in this study. First, there was a small number of animals due to ethical issues. Second, only female mice were included because many male mice died due to the intrauterine ischemia. The results of male mice showed a similar trend; however, the relationship was not as significant as those of females. Fewer male mice used in the experiments may have contributed to a less significant difference. Mitochondria are maternally inherited and may be more likely to appear as a female phenotype; however, further studies are needed using large sample sizes in both sexes. Third, visceral fat accumulation was not assessed by any imaging. Fourth, intrauterine ischemia is a cause of LBW at birth, but not of all LBW causes. Finally, since the equation of HOMA-R generally use is for humans, it is necessary to verify whether the results of this formula really represent insulin resistance in mice.

5. Conclusions

This mouse model showed non-obese hyperglycemia in young adulthood after birth with LBW due to transient intrauterine ischemia. A pathogenetic mechanism may involve increased myogenic insulin resistance by mitochondrial dysfunction. In the future, using this model, preventive and therapeutic strategies for non-obese hyperglycemia will be studied, such as the use of growth hormone, whey protein, or Chinese medicine, and non-invasive insulin therapy [50].

6. Patents

A method for producing a mouse model that develops non-obese type 2 diabetic in young adulthood after birth with LBW due to transient intrauterine ischemia was lodged with the Japanese Patent Office on 6 July 2020, by Nobuhiko Nagano, Ichiro Morioka, Shoichi Shimizu, and Daichi Katayama (application number: 2020-116354).

References

1. Barker, D.J.; Osmond, C. Infant mortality, childhood nutrition, and ischaemic heart disease in England and Wales. *Lancet* **1986**, *1*, 1077–1081. [CrossRef]
2. Gluckman, P.D.; Hanson, M.A. Living with the past: Evolution, development, and patterns of disease. *Science* **2004**, *305*, 1733–1736. [CrossRef]
3. De Boo, H.A.; Harding, J.E. The developmental origins of adult disease (Barker) hypothesis. *Aust. N. Z. J. Obstet. Gynaecol.* **2006**, *46*, 4–14. [CrossRef] [PubMed]
4. Ministry of Health, Labor and Welfare in Japan. Vital Statistics in Japan in 2017. Available online: https://www.mhlw.go.jp/toukei/list/81-1.html (accessed on 7 June 2022). (In Japanese)
5. The World Bank. Low-Birthweight Babies (% of Birth). Available online: https://data.worldbank.org/indicator/SH.STA.BRTW.ZS (accessed on 6 June 2022).
6. Kuwabara, R.; Urakami, T.; Yoshida, K.; Morioka, I. Case of type 2 diabetes possibly caused by excessive accumulation of visceral fat in a child born small-for-gestational age. *J. Diabetes Investig.* **2020**, *11*, 1366–1369. [CrossRef] [PubMed]
7. Sone, H.; Ito, H.; Ohashi, Y.; Akanuma, Y.; Yamada, N.; Japan Diabetes Complication Study Group. Obesity and type 2 diabetes in Japanese patients. *Lancet* **2003**, *361*, 85. [CrossRef]
8. The Examination Committee of Criteria for 'Obesity Disease' in Japan; Japan Society for the Study of Obesity. New criteria for 'obesity disease' in Japan. *Circ. J.* **2002**, *66*, 987–992. [CrossRef]
9. Urakami, T.; Morimoto, S.; Nitadori, Y.; Harada, K.; Owada, M.; Kitagawa, T. Urine glucose screening program at schools in Japan to detect children with diabetes and its outcome-incidence and clinical characteristics of childhood type 2 diabetes in Japan. *Pediatr. Res.* **2007**, *61*, 141–145. [CrossRef]
10. Simmons, R.A.; Templeton, L.J.; Gertz, S.J. Intrauterine growth retardation leads to the development of type 2 diabetes in the rat. *Diabetes* **2001**, *50*, 2279–2286. [CrossRef]
11. Takeno, K.; Tamura, Y.; Kawaguchi, M.; Kakehi, S.; Watanabe, T.; Funayama, T.; Furukawa, Y.; Kaga, H.; Yamamoto, R.; Kim, M.; et al. Relation between insulin sensitivity and metabolic abnormalities in Japanese men with BMI of 23–25 kg/m^2. *J. Clin. Endocrinol. Metab.* **2016**, *101*, 3676–3684. [CrossRef]
12. Spalding, K.L.; Arner, E.; Westermark, P.O.; Bernard, S.; Buchholz, B.A.; Bergmann, O.; Blomqvist, L.; Hoffstedt, J.; Näslund, E.; Britton, T.; et al. Dynamics of fat cell turnover in humans. *Nature* **2008**, *453*, 783–787. [CrossRef]

13. Kubo, K.-I.; Deguchi, K.; Nagai, T.; Ito, Y.; Yoshida, K.; Endo, T.; Benner, S.; Shan, W.; Kitazawa, A.; Aramaki, M.; et al. Association of impaired neuronal migration with cognitive deficits in extremely preterm infants. *JCI Insight* **2017**, *2*, e88609. [CrossRef] [PubMed]

14. Kimura, K.; Takeuchi, K. Growth of the Jcl: ICR mouse. *Okajimas Folia Anat. Jpn.* **1986**, *63*, 265–280. [CrossRef] [PubMed]

15. Matthews, D.R.; Hosker, J.P.; Rudenski, A.S.; Naylor, B.A.; Treacher, D.F.; Turner, R.C. Homeostasis model assessment: Insulin resistance and beta-cell function from fasting plasma glucose and insulin concentrations in man. *Diabetologia* **1985**, *28*, 412–419. [CrossRef] [PubMed]

16. Lukaski, H.C.; Johnson, P.E.; Bolonchuk, W.W.; Lykken, G.I. Assessment of fat free mass using bioelectrical impedance measurements of the human body. *Am. J. Clin. Nutr.* **1985**, *41*, 810–817. [CrossRef]

17. Okazaki, M.; Yamashita, S. Recent advances in analytical methods on lipoprotein subclasses: Calculation of particle numbers from lipid levels by gel permeation HPLC using "Spherical Particle Model". *J. Oleo Sci.* **2016**, *65*, 265–282. [CrossRef]

18. Usui, S.; Hara, Y.; Hosaki, S.; Okazaki, M. A new on-line dual enzymatic method for simultaneous quantification of cholesterol and triglycerides in lipoproteins by HPLC. *J. Lipid Res.* **2002**, *43*, 805–814. [CrossRef]

19. Okazaki, M.; Usui, S.; Ishigami, M.; Sakai, N.; Nakamura, T.; Matsuzawa, Y.; Yamashita, S. Identification of unique lipoprotein subclasses for visceral obesity by component analysis of cholesterol profile in high-performance liquid chromatography. *Arterioscler. Thromb. Vasc. Biol.* **2005**, *25*, 578–584. [CrossRef]

20. Ohashi, Y.; Hirayama, A.; Ishikawa, T.; Nakamura, S.; Shimizu, K.; Ueno, Y.; Tomita, M.; Soga, T. Depiction of metabolome changes in histidine-starved *Escherichia coli* by CE-TOFMS. *Mol. Biosyst.* **2008**, *4*, 135–147. [CrossRef]

21. Ooga, T.; Sato, H.; Nagashima, A.; Sasaki, K.; Tomita, M.; Soga, T.; Ohashi, Y. Metabolomic anatomy of an animal model revealing homeostatic imbalances in dyslipidaemia. *Mol. Biosyst.* **2011**, *7*, 1217–1223. [CrossRef]

22. Sugimoto, M.; Wong, D.T.; Hirayama, A.; Soga, T.; Tomita, M. Capillary electrophoresis mass spectrometry-based saliva metabolomics identified oral, breast and pancreatic cancer-specific profiles. *Metabolomics* **2010**, *6*, 78–95. [CrossRef]

23. Yamamoto, H.; Fujimori, T.; Sato, H.; Ishikawa, G.; Kami, K.; Ohashi, Y. Statistical hypothesis testing of factor loading in principal component analysis and its application to metabolite set enrichment analysis. *BMC Bioinform.* **2014**, *15*, 51. [CrossRef] [PubMed]

24. Junker, B.H.; Klukas, C.; Schreiber, F. VANTED: A system for advanced data analysis and visualization in the context of biological networks. *BMC Bioinform.* **2006**, *7*, 109. [CrossRef] [PubMed]

25. Wigglesworth, J.S. Experimental growth retardation in the foetal rat. *J. Pathol. Bacteriol.* **1964**, *88*, 1–13. [CrossRef] [PubMed]

26. Garofano, A.; Czernichow, P.; Breant, B. In utero undernutrition impairs rat beta-cell development. *Diabetologia* **1997**, *40*, 1231–1234. [CrossRef] [PubMed]

27. Ozaki, T.; Nishina, H.; Hanson, M.A.; Poston, L. Dietary restriction in pregnant rats causes gender-related hypertension and vascular dysfunction in offspring. *J. Physiol.* **2001**, *530*, 141–152. [CrossRef]

28. Jimenez-Chillaron, J.C.; Hernandez-Valencia, M.; Reamer, C.; Fisher, S.; Joszi, A.; Hirshman, M.; Oge, A.; Walrond, S.; Przybyla, R.; Boozer, C.; et al. β-cell secretory dysfunction in the pathogenesis of low birth weight-associated diabetes: A murine model. *Diabetes* **2005**, *54*, 702–711. [CrossRef]

29. Ogata, E.S.; Bussey, M.E.; Finley, S. Altered gas exchange, limited glucose and branched chain amino acids, and hypoinsulinism retard fetal growth in the rat. *Metabolism* **1986**, *35*, 970–977. [CrossRef]

30. Ylihärsilä, H.; Kajantie, E.; Osmond, C.; Forsén, T.; Barker, D.J.; Eriksson, J.G. Birth size, adult body composition and muscle strength in later life. *Int. J. Obes.* **2007**, *31*, 1392–1399. [CrossRef]

31. Matinolli, H.M.; Hovi, P.; Männistö, S.; Sipola-Leppänen, M.; Eriksson, J.G.; Mäkitie, O.; Järvenpää, A.L.; Andersson, S.; Kajantie, E. Early protein intake is associated with body composition and resting energy expenditure in young adults born with very low birth weight. *J. Nutr.* **2015**, *145*, 2084–2091. [CrossRef]

32. Cho, W.K.; Suh, B.K. Catch-up growth and catch-up fat in children born small for gestational age. *Korean J. Pediatr.* **2016**, *59*, 1–7. [CrossRef]

33. Feng, Z.; Hanson, R.W.; Berger, N.A.; Trubitsyn, A. Reprogramming of energy metabolism as a driver of aging. *Oncotarget* **2016**, *7*, 15410–15420. [CrossRef] [PubMed]

34. Imai, S.-I.; Guarente, L. NAD$^+$ and sirtuins in aging and disease. *Trends Cell Biol.* **2014**, *24*, 464–471. [CrossRef] [PubMed]

35. Granger, D.N.; Kvietys, P.R. Reperfusion injury and reactive oxygen species: The evolution of a concept. *Redox Biol.* **2015**, *6*, 524–551. [CrossRef]

36. Crabtree, M.J.; Hale, A.B.; Channon, K.M. Dihydrofolate reductase protects endothelial nitric oxide synthase from uncoupling in tetrahydrobiopterin deficiency. *Free Radic. Biol. Med.* **2011**, *50*, 1639–1646. [CrossRef] [PubMed]

37. Rasola, A.; Bernardi, P. The mitochondrial permeability transition pore and its involvement in cell death and in disease pathogenesis. *Apoptosis* **2007**, *12*, 815–833. [CrossRef]

38. Yu, N.; Wang, S.; Wang, P.; Li, Y.; Li, S.; Chen, H.; Wang, T. The calcium uniporter regulates the permeability transition pore in isolated cortical mitochondria. *Neural Regen. Res.* **2012**, *7*, 109–113. [CrossRef]

39. Sangwung, P.; Petersen, K.F.; Shulman, G.I.; Knowles, J.W. Mitochondrial dysfunction, insulin resistance, and potential genetic implications. *Endocrinology* **2020**, *161*, bqaa017. [CrossRef]

40. Zhao, Y.; Zhang, Y.; Qi, M.; Ping, F.; Zhang, H.; Xu, L.; Li, W.; Li, Y. The role of lactate exercise test and fasting plasma c-peptide levels in the diagnosis of mitochondrial diabetes: Analysis of clinical characteristics of 12 patients with mitochondrial diabetes in a single center with long-term follow-up. *Front. Endocrinol.* **2022**, *13*, 835570. [CrossRef]

41. Petersen, K.F.; Befroy, D.; Dufour, S.; Dziura, J.; Ariyan, C.; Rothmann, D.L.; DiPietro, L.; Cline, G.W.; Shulman, G.I. Mitochondrial dysfunction in the elderly: Possible role in insulin resistance. *Science* **2003**, *300*, 1140–1142. [CrossRef]

42. Petersen, K.F.; Dufour, S.; Befroy, D.; Garcia, R.; Shulman, G.I. Impaired mitochondrial activity in the insulin-resistant offspring of patients with type 2 diabetes. *N. Engl. J. Med.* **2004**, *350*, 664–671. [CrossRef]

43. Kelley, D.E.; He, J.; Menshikova, E.V.; Ritov, V.B. Dysfunction of mitochondria in human skeletal muscle in type 2 diabetes. *Diabetes* **2002**, *51*, 2944–2950. [CrossRef] [PubMed]

44. Toledo, F.G.; Menshikova, E.V.; Ritov, V.B.; Azuma, K.; Radikova, Z.; DeLany, J.; Kelley, D.E. Effects of physical activity and weight loss on skeletal muscle mitochondria and relationship with glucose control in type 2 diabetes. *Diabetes* **2007**, *56*, 2142–2147. [CrossRef] [PubMed]

45. Song, J.; Oh, J.Y.; Sung, Y.A.; Pak, Y.; Park, K.S.; Lee, H.K. Peripheral blood mitochondrial DNA content is related to insulin sensitivity in offspring of type 2 diabetic patients. *Diabetes Care* **2001**, *24*, 865–869. [CrossRef] [PubMed]

46. Wang, X.; Li, H.; Zheng, A.; Yang, L.; Liu, J.; Chen, C.; Tang, Y.; Zou, X.; Li, Y.; Long, J.; et al. Mitochondrial dysfunction-associated OPA1 cleavage contributes to muscle degeneration: Preventative effect of hydroxytyrosol acetate. *Cell Death Dis.* **2014**, *5*, e1521. [CrossRef] [PubMed]

47. Sugiyama, S.; Jinnouchi, H.; Hieshima, K.; Kurinami, K.; Jinnouchi, K. A non-obese, treatment-naive Japanese diabetic patient with elevated insulin clearance and hyperglycemia under enhanced insulin sensitivity and increased insulin secretion: Elevated insulin clearance as type 2 Japanese diabetes mellitus (T2JDM). *Cureus* **2021**, *13*, e14354. [CrossRef]

48. Furuta, M.; Tamai, M.; Hanabusa, T.; Yamamoto, Y.; Nanjo, K.; Sanke, T. Serum adiponectin is associated with fasting serum C-peptide in non-obese diabetic patients. *Diabetes Res. Clin. Pract.* **2006**, *72*, 302–307. [CrossRef]

49. Rattarasarn, C. Dysregulated lipid storage and its relationship with insulin resistance and cardiovascular risk factors in non-obese Asian patients with type 2 diabetes. *Adipocyte* **2018**, *7*, 71–80. [CrossRef]

50. Sabbagh, F.; Muhamad, I.I.; Niazmand, R.; Dikshit, P.K.; Kim, B.S. Recent progress in polymeric non-invasive insulin delivery. *Int. J. Biol. Macromol.* **2022**, *203*, 222–243. [CrossRef]

論文の内容の要旨

氏名：片山大地

博士の専攻分野の名称：博士（医学）

論文題名：A Non-Obese Hyperglycemic Mouse Model that Develops after Birth with Low Birthweight

（低出生体重-非肥満型高血糖発症マウスモデル）

1 背景と目的

　胎児期に低栄養に暴露された胎児は、低体重で出生し、子宮内の低栄養環境への適応を通じてエネルギー効率の高い脂肪を蓄積しやすい倹約型の体質を獲得する [1, 2]。そして、出生後に児の栄養環境が改善すると相対的な過栄養状態となるため、成人期に 2 型糖尿病などの生活習慣病を発症するリスクが高くなることが提唱された（Developmental Origins of Health and Disease: DOHaD 説)[3]。日本では総出生数は減少しているが、超低出生体重児など救命困難な児も救命できるようになったため出生体重が 2500g 未満の低出生体重児は減少していない [4]。そのため我が国では、低出生体重児の将来の健康障害を減らすことが医療的・経済的・社会的に求められている。DOHaD 説に関連するアニマルモデルはいくつか報告されている。妊娠中のマウスにおける両側子宮動脈の結紮や妊娠中の栄養制限などの子宮内低栄養は、胎児の成長抑制を引き起こす可能性がある [5−8]。また、成人期の肥満で高血糖を発症するアニマルモデルや [9]、成人期に低体重のままであるが高血糖を発症しないアニマルモデルがある [10]。一方、実臨床では低体重で出生した一部の児は著明な肥満を伴わずに糖尿病を発症する症例が存在するが [11]、このような肥満を伴わない 2 型糖尿病アニマルモデルは現在まで存在しない。本研究は、①子宮内虚血マウスモデルが低体重で出生後、将来的に非肥満型高血糖を発症するかどうかを検討すること、②非肥満型高血糖発症の機序を解明することを目的とした。

2 方法

2.1 研究デザイン、プロトコール及び動物モデル

　全てのプロトコールと手順は、日本大学医学部動物実験委員会の承認を受け実施した(承認番号： AP18MED033-1, 承認日 2019 年 7 月 5 日, 承認番号： AP20MED003-1, 承認日 2020 年 4 月 3 日)。ICR 系統の妊娠マウスを妊娠 16.5 日にイソフルラン麻酔下で下腹部を切開した。両側子宮動脈の血流をクリップで遮断し、胎児の低酸素と低栄養を引き起こした群を虚血群（I）とした(図 1 a)。15 分後クリップを外し、胎仔を腹腔内に還納、腹部を縫合した。同様の麻酔下で下腹部の切開のみを行った群をコントロール群（C）とした。出生した I 群と C 群の雌の新生仔を 4 週齢で離乳し、8 週齢まで普通食で飼育した（各群：n=7）。体重測定は出生時と 8 週齢まで週 2 回行った。8 週齢で 12 時間絶食後、体組成の測定（図 1c）を行い、心臓から採血し、肝臓を摘出した(図 1b)。雌の空腹時血糖値、血清インスリン濃度(immunoreactive insulin: IRI)、インスリン抵抗指数(homeostasis model

assessment of insulin resistance: HOMA-R)、体組成（脂肪量、除脂肪量）、血清コレステロール濃度、中性脂肪を2群間で比較した（各群 n=7）。また、摘出した肝臓のメタボローム解析を施行した（各群 n=3）。

2.2 グルコース代謝
　8週齢の成獣マウスを12時間絶食後、血糖値、IRI を測定した。HOMA-R はマウス用の式がないためヒト用の式、空腹時血糖(mg/dl)×血清 IRI 濃度（μIU）/405 により算出した。

2.3 体組成
　体組成はインピーダンス法を用い体脂肪率と除脂肪率を測定した。そして、(1)体脂肪量(g)および(2)除脂肪量(g)は、以下の式で計算した。

$$(1)体脂肪量(g)＝8週齢体重(g)×体脂肪率/100$$
$$(2)除脂肪量(g)＝8週齢体重(g)×除脂肪率/100$$

2.4 血清リポタンパク質濃度
　血清リポタンパク質中のコレステロールおよびトリグリセリドのプロファイルはゲルろ過高速液体クロマトグラフィー法（LipoSEARCH®; Skylight Biotech、秋田、日本）を使用して解析を行った[12-14]。

2.5 肝臓のメタボローム解析
　妊娠マウスから出生し、8週齢となったマウスの肝臓（各群 n=3）を用いてメタボローム解析を行った。

2.6 統計学的解析
　データは、平均±平均の標準誤差で表示した。2群間の比較は必要に応じて JMP ver.14 を使用して、Mann-Whitney U 検定または Welch の t 検定を行った。p 値＜0.05 を有意差ありとした。

3 結果
3.1 出生体重、体重推移
　出生体重の平均値は I 群 1.5g、C 群 1.8g と子宮内虚血によって低出生体重仔が産まれた（p<0.05）（図 2a）。その後も I 群は低体重で推移し、8週齢でも平均体重 I 群 35.5g、C 群 40.2g と I 群は低体重のまま推移した（p<0.05）(図 2b)。

3.2 グルコース代謝
　8週齢の平均空腹時血糖値は、C 群と比較して I 群で有意に高かった(I 群 196.9 vs C 群

75.0mg/dL、p<0.01)。IRI および HOMA-R の平均値は、C 群(1.4µIU/m、0.3)と比較して、I 群(3.9µIU/mL、1.9)で有意に高かった(それぞれ p<0.05、p<0.01)(表 1)。

3.3 体組成
I 群および C 群の平均脂肪重量(I 群 16.6 vs C 群 17.7g)の間に有意差はなかった(p=0.95)。一方、平均除脂肪量は、C 群よりも I 群で有意に低かった(I 群 19.1 vs C 群 22.6g、p<0.05) (表 2)。

3.4 血清リポタンパク質濃度
総コレステロール、LDL(low density lipoprotein)コレステロール、VLDL(very low density lipoprotein)コレステロール、および HDL(high density lipoprotein)コレステロールの平均値は I 群でそれぞれ 104.4mg/dL、15.5mg/dL、10.7mg/dL、77.6mg/dL、C 群で 99.3mg/dL、16.5mg/dL、8.2mg/dL、74.3mg/dL でありいずれも 2 群間で有意差はなかった。中性脂肪は C 群(37.3mg/dL)よりも I 群 (88.1mg/dL) で有意に高かった (p<0.05) (表 2)。

3.5 メタボローム解析
肝臓のメタボローム解析では、TCA 回路の中間代謝産物であるリンゴ酸、フマル酸は C 群よりも I 群で有意に高く(それぞれ p<0.001、p<0.001)、ニコチンアミドアデニンジヌクレオチド(nicotinamide adenine dinucleotide: NAD+)およびアデノシン三リン酸(adenosine triphosphate: ATP)は、C 群よりも I 群において有意に低かった（それぞれ p<0.05、p<0.05)。一方、乳酸は C 群よりも I 群で有意に高かった(p<0.01)（表 3、図 3)。この結果からミトコンドリア機能低下の存在が示唆された。また、代表的な酸化ストレスマーカーである 3-インドキシル硫酸、システイン、および S アデノシルメチオニンは I 群で C 群よりも有意に高かった(それぞれ p<0.001、p<0.05、p<0.01)(表 4)。

4.考察
実臨床では低体重で生まれた児は、著名な肥満を伴わずに糖尿病を発症する症例が存在している [11]。しかしこのような動物モデルはまだ開発されていない。 本研究では、妊娠マウスの子宮動脈の血流を一時的に遮断することにより、低体重で出生し、若年成人期に非肥満型高血糖をもたらすことを確認した。 総コレステロール、LDL コレステロール、VLDL コレステロール、および HDL コレステロールは 2 郡間で有意な差はなかった。 除脂肪量の減少とミトコンドリア機能低下による筋原性インスリン抵抗性が非肥満型高血糖の発症に関与していると考えられた。(図 4)。

4.1 筋原性インスリン抵抗性
I 群は C 群よりも除脂肪量が有意に低かったが、2 群間で脂肪量に差はなかった。低出生

体重で生まれた児は、成人期の筋肉量が少ない傾向があり[15]、基礎代謝が低い[16]ため、内臓脂肪の蓄積、アディポネクチン分泌の減少、およびインスリン抵抗性につながる[17]。本研究の動物モデルは、筋肉量の減少による筋原性インスリン抵抗性を示した。これは非肥満型高血糖の原因の一つと考えられる。

4.2 ミトコンドリア機能低下

　ミトコンドリアはATPなどのエネルギー生産の場所である。したがって、ミトコンドリアの機能低下はATP産生を減少させる。ATPは嫌気的解糖によって生成されるため、乳酸が増加する[18]。 NAD+はミトコンドリアにおけるエネルギー生産の補因子の1つであり、ミトコンドリアの機能低下によって減少する[19]。 本研究では、メタボローム解析により、I群のATP産生の減少、乳酸の増加、および NAD+の減少によるミトコンドリア機能低下が示された。さらに、酸化ストレスである3-インドキシル硫酸は、C群と比較してI群で有意に高かった。虚血と再灌流は活性酸素などの酸化ストレスを引き起こし、ミトコンドリア機能低下をもたらす[20-23]。本マウスモデルも同じメカニズムでミトコンドリア機能低下を引き起こした可能性がある。ミトコンドリア機能低下は、それ自体でもインスリン抵抗性を引きし、高血糖を発症する[24]。また、ミトコンドリア機能低下は筋萎縮を引き起こし[25]、筋肉量の減少によるインスリン抵抗性と関連している可能性がある。

　ミトコンドリア機能低下はインスリン分泌障害、インスリン抵抗性いずれも引き起こす。本研究では虚血群でインスリン分泌が亢進し、ＨＯＭＡ－Ｒが高値であったことからインスリン抵抗性が高血糖をもたらしていると考えた。しかし、インスリン分泌障害も生じておりインスリンが相対的に不足していることや、インスリン抵抗性の両方が高血糖の原因となっている可能性もある。そのため膵臓のインスリン含有量の評価、ピルビン酸負荷試験による血糖推移からインスリン分泌の評価やインスリン負荷試験によるインスリン抵抗性の評価が必要である。また、メタボローム解析で虚血群はホスホエノールピルビン酸からピルビン酸の産生が低下している。この代謝に関わる酵素であるピルビン酸キナーゼの発現に関与するPVLR遺伝子の異常をきたしている可能性がある。

研究の限界

　本研究では倫理的な問題から検討できたマウスの数が充分ではなかった。雄のマウスの結果も同様な傾向であったが、雌のマウスで違いが顕著であった。これは検体数の少なさが影響した可能性がある。そのため雄雌いずれも検体数を増やして更なる検討が必要である。また、筋肉量が減少し、筋原性インスリン抵抗性に関与する遺伝子を欠損させたマウスが非肥満型高血糖を発症するか検討する必要がある。

5 結論

　子宮内虚血によって低出生体重で出生し、成獣期に非肥満型高血糖を発症するマウスモデルを開発した（特許出願中 2020-116354）。高血糖発症の機序は、ミトコンドリア機能低下と除脂肪量の減少に基づく筋原性インスリン抵抗性の増加による可能性がある。

6 今後の展望

　本マウスモデルは低出生体重で出生し、成獣期に非肥満型高血糖をきたす世界初の動物モデルであり、本研究のマウスモデルを用いて、低出生体重-非肥満型高血糖の発症予防や治療法の開発研究を行うことが可能となる。その結果、低出生体重児の成人期の健康増進に大きく貢献できる可能性がある。
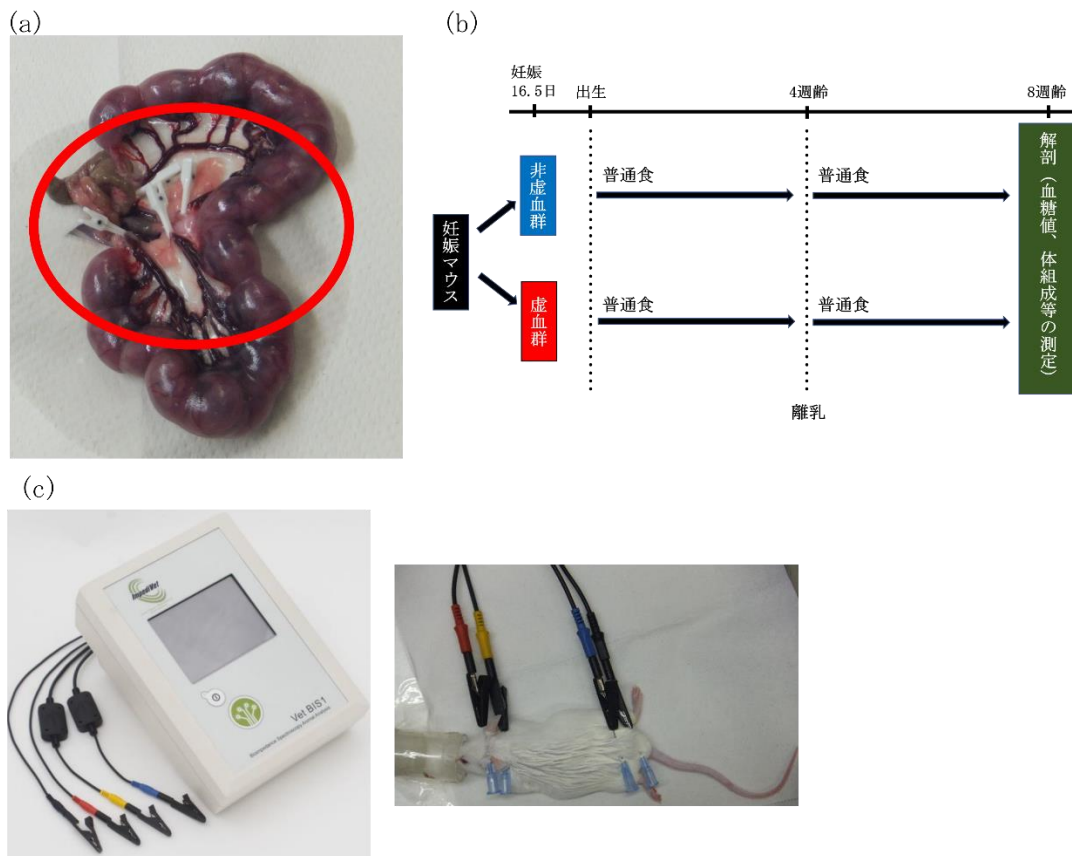
図1　実験手順（a）両側子宮動脈の遮断、（b）本研究の流れ、（C)体組成の測定。
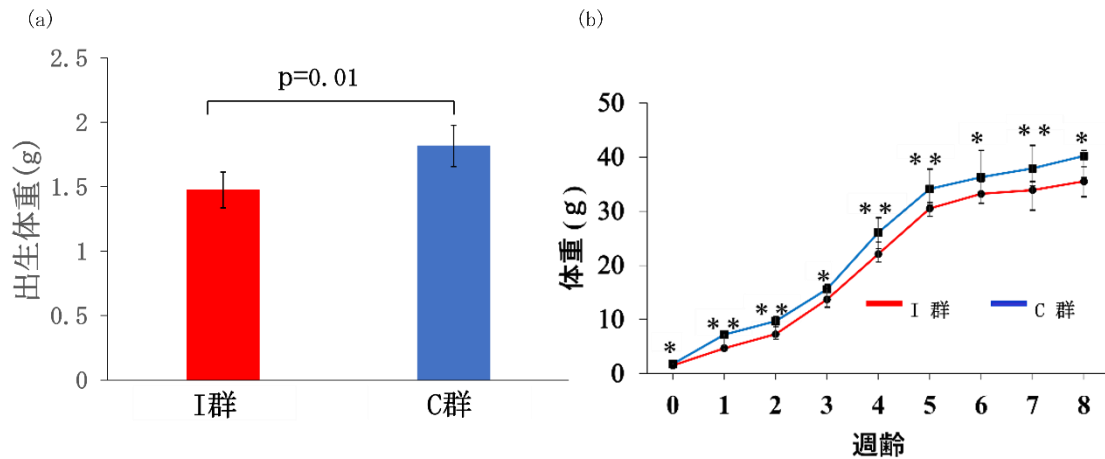
図2 (a) 出生体重(b) 出生から 8 週齢までの体重推移。平均±標準誤差(各群 n=7)、*p ＜ 0.05、
**p ＜ 0.01。

表1　グルコース代謝

	コントロール群(n=7)	虚血群(n=7)	p-Value
血糖値（mg/dL）	75.0±4.8	196.9±17.7	＜0.01
IRI（μIU/mL）	1.4±0.4	3.9±1.0	＜0.05
HOMA-R	0.3±0.1	1.9±0.4	＜0.01

Data are shown as the mean ± standard error of the mean (n = 7 per group)

HOMA-R: homeostasis model assessment of insulin resistance、

IRI: immunoreactive insulin

表2　体組成、血清リポタンパク質濃度

	コントロール群(n=7)	虚血群(n=7)	p-Value
脂肪量（g）	17.7±0.9	16.6±1.9	0.95
除脂肪量（g）	22.6±0.8	19.1±1.6	＜0.05
総コレステロール（mg/dL）	99.3±3.1	104.4±8.5	0.91
LDL コレステロール（mg/dL）	16.5±1.2	15.5±2.3	0.40
VLDL コレステロール（mg/dL）	8.2±0.9	10.7±1.4	0.07
HDL コレステロール（mg/dL）	74.3±1.8	77.6±6.7	0.60
中性脂肪（mg/dL）	37.3±5.5	88.1±13.6	＜0.05

Data are shown as the mean ± standard error of the mean (n = 7 per group)

LDL: low density lipoprotein、VLDL: very low density lipoprotein、HDL: high
density lipoprotein

表3　肝臓のメタボローム解析

	コントロール群(n=3)	虚血群(n=3)	p-Value
リンゴ酸（nmol/g）	508±96	2188±50	＜0.001
フマル酸（nmol/g）	308±41	829±34	＜0.001
ATP（nmol/g）	35±6.5	16±1.6	＜0.05
NAD+	31±5.5	60±8.1	＜0.05
乳酸（nmol/g）	5200±1100	15600±1700	＜0.01

Data are shown as the mean ± standard error of the mean (n = 7 per group)
ニコチンアミドアデニンジヌクレオチド(nicotinamide adenine dinucleotide: NAD+)、
アデノシン三リン酸（adenosine triphosphate: ATP）

表4　酸化ストレス

		コントロール群 vs. 虚血群	
		比*	p-Value
酸化ストレス	インドキシル硫酸	2.0	＜0.001
	システイン	3.0	＜0.05
	S-アデノシルメチオニン	1.7	＜0.01
	エルゴチオネイン	0.7	0.061
	N,N-ジメチルグリシン	0.9	0.683

Data are shown as the mean ± standard error of the mean (n = 7 per group)
*2群間の平均値の比。

a

Pyruvic acid Lactic acid

Glu
Asp
2-OG

CoASH   NAD+
CO$_2$ NADH
H+

Pyruvate
dehydrogenase
kinase

Oxaloacetate

Citrate lyase

ATP
HCO$_3^-$
Pyruvate
carboxylase
ADP

Pyruvate
dehydrogenase

ATP
CoA
H$_2$O

H+
NADH

Oxaloacetate

AcCoA   H$_2$O

CoASH

Citrate
synthase

CoA

AD+

Malate
dehydrogenase

Malic acid

Citric acid   H$_2$O

TCA cycle

Aconitase

cis-Aconitic acid

H$_2$O

Fumarase

Aconitase

Fumaric acid

Succinate
dehydrogenase

Isocitric acid

DH
FAD

Succinyl-CoA
synthetase

Isocitrate
dehydrogenase

NAD+
NADH
H+
CO$_2$

Succinic acid

GTP GDP
CoASH Pi

Oxoglutarate
dehydrogenase

SucCoA

NADH
H+
CO$_2$

NAD+
CoASH

2-OG

Glu   G

ide Mitochondria

Isocitrate
dehydrogenase
(mutant)

Mitochondrial m
dehydrogena

2-OG

NADH

Malic acid

2-Hydroxygl
dehydrogena

2-OG

FADH$_2$

2-Hydroxyglutaric acid

ADP   ATP

H+
NADH   NAD+

Respiratory chain

GTP GDP

CoQ

ETC
NADH
dehydrogenase

DH$_2$ FAD

ETC
Succinate
dehydrogenase

H+

ETC
Cytochrome bcI
complex

CytC

ETC
Cytochrome c
oxidase

H+
ATP
synthase

Fo

H+
ATP

case
ADP ATP   H+   H+

ATP

b

図3 （a）ミトコンドリア内のクエン酸回路。（b）解糖系。

Lactic acid:乳酸、Malic acid:リンゴ酸、Fumaric acid:フマル酸、アデノシン三リン酸
（adenosine triphosphate: ATP）、ニコチンアミドアデニンジヌクレオチド(nicotinamide
adenine dinucleotide: NAD+)。
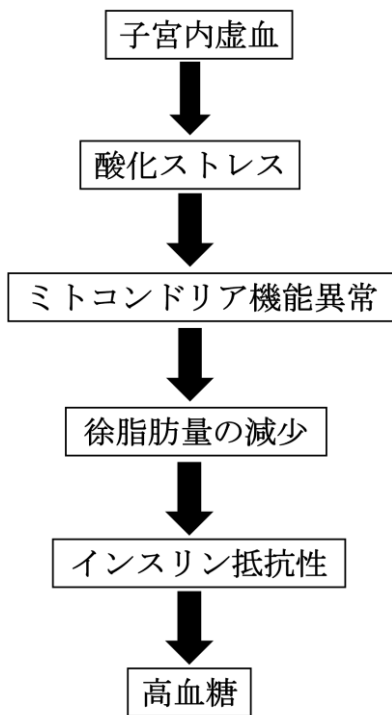
図 4 本モデルにおける低出体重で出生後、非肥満性高血糖を発症する機序
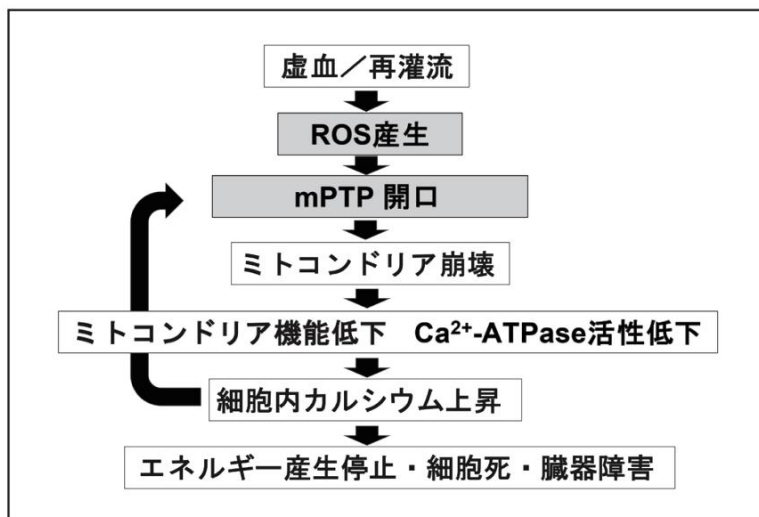
図 5 虚血および再灌流によるミトコンドリア機能低下
ミトコンドリア透過性遷移孔(mitochondrial permeability pore: mPTP)、活性酸素種
(reactive oxygenspecies: ROS)。

メタボローム解析その他の結果

1.

Supplementary Table S1. Principal component score

	Contribution rate (%)	Group I			Group C		
		I1	I2	I3	C1	C2	C3
PC1	41.99	-12.09	-11.01	-7.41	9.73	11.66	9.12
PC2	18.80	-4.70	-0.08	6.81	7.68	2.58	-12.28
PC3	15.49	8.01	0.62	-10.21	2.82	4.72	-5.97
PC4	13.40	-6.54	10.96	-5.23	2.57	-2.39	0.63
PC5	10.32	-2.56	2.77	0.94	-8.02	8.60	-1.73

PC, principal component

Supplementary Table S2. Metabolites and principal component score

	Compound name	PubChem CID	HMDB ID	m/z	MT/RT	PC1	PC2
A_0003	Pyruvic acid	1060	HMDB0000243	87.009	10.49	9.9E-01	-2.2E-02
A_0004	Butyric acid Isobutyric acid	264 6590	HMDB0000039 HMDB0001873	87.045	8.31	-3.2E-01	4.4E-01
A_0005	Lactic acid	612	HMDB0000190,HMDB0001311	89.024	9.00	-9.5E-01	1.3E-01
A_0006	3-Hydroxybutyric acid	441	HMDB0000011,HMDB0000357,HMDB0000442	103.039	8.04	8.6E-01	3.4E-01
A_0007	2-Hydroxybutyric acid	440864	HMDB0000008	103.040	8.24	7.4E-01	5.3E-01
A_0008	Fumaric acid	444972	HMDB0000134	115.003	17.57	-9.8E-01	3.3E-02
A_0010	Succinic acid	1110	HMDB0000254	117.019	15.52	-5.5E-01	4.3E-01
A_0011	β-Hydroxyisovaleric acid	69362	HMDB0000754	117.056	7.63	2.3E-01	1.3E-01
A_0012	XA0003			124.991	10.24	-5.3E-01	-7.9E-01
A_0013	Isethionic acid	7866	HMDB0003903	124.991	9.55	8.1E-01	2.2E-01
A_0014	5-Oxoproline	7405	HMDB0000267	128.035	7.97	9.1E-01	-1.1E-01
A_0015	N-Acetylalanine	88064	HMDB0000766	130.051	7.50	-7.9E-01	4.2E-01
A_0016	Malic acid	525	HMDB0000156,HMDB0000744	133.013	15.73	-9.9E-01	3.5E-02
A_0017	Threonic acid	5460407	HMDB0000943	135.030	7.79	4.7E-01	4.2E-01
A_0018	Ethanolamine phosphate	1015	HMDB0000224	140.011	6.79	8.9E-01	4.0E-01
A_0019	Octanoic acid	379	HMDB0000482	143.107	7.11	4.2E-01	5.0E-01
A_0020	4-Acetamidobutanoic acid	18189	HMDB0003681	144.066	7.29	5.1E-01	1.7E-01
A_0022	2-Hydroxyglutaric acid	43	HMDB0000606,HMDB0000694	147.029	13.32	-8.6E-01	-2.6E-01
A_0023	Cysteinesulfinic acid	1549098	HMDB0000996	152.000	8.01	9.0E-01	-2.9E-01
A_0024	Pelargonic acid	8158	HMDB0000847	157.123	6.93	2.6E-01	5.3E-01
A_0025	Terephthalic acid	7489	HMDB0002428	165.018	13.08	-4.1E-01	-2.7E-01
A_0026	XA0012			166.018	7.89	4.2E-01	-4.0E-01
A_0027	Phosphoenolpyruvic acid	1005	HMDB0000263	166.974	15.58	6.7E-01	-5.9E-01
A_0028	Uric acid	1175	HMDB0000289	167.021	7.50	6.8E-01	6.7E-01
A_0029	Dihydroxyacetone phosphate	668	HMDB0001473	168.990	10.43	-9.6E-01	-7.7E-02
A_0030	Glyceraldehyde 3-phosphate	729	HMDB0001112	168.991	9.66	-5.3E-01	-3.0E-01
A_0031	Glycerol 3-phosphate	439162	HMDB0000126	171.006	10.00	-6.8E-02	3.3E-01
A_0032	Decanoic acid	2969	HMDB0000511	171.140	6.77	2.9E-01	-1.2E-01
A_0033	Isovalerylalanine N-Acetylleucine	129285 70912	HMDB0000747 HMDB0011756	172.097	6.80	-3.8E-01	-6.1E-02
A_0035	N-Acetylasparagine	99715	HMDB0006028	173.057	7.11	1.6E-01	5.2E-01
A_0036	Suberic acid	10457	HMDB0000893	173.084	10.57	-3.0E-01	3.7E-01
A_0037	N-Acetylaspartic acid	65065	HMDB0000812	174.041	11.76	-9.1E-02	6.9E-01
A_0038	Ascorbic acid	54670067	HMDB0000044	175.024	7.18	-3.3E-02	7.0E-01
A_0039	Allantoic acid	203	HMDB0001209	175.046	7.33	-1.3E-01	-4.2E-01
A_0040	3-Phosphoglyceric acid	439183	HMDB0000807	184.984	14.82	7.1E-01	9.6E-02
A_0042	XA0017			186.114	6.68	6.0E-01	-7.0E-03
A_0043	N-Acetylglutamine	25561	HMDB0006029	187.073	6.86	-7.9E-01	5.7E-02
A_0044	Azelaic acid	2266	HMDB0000784	187.097	10.07	-2.9E-01	4.3E-01
A_0045	N-Acetylglutamic acid	70914	HMDB0001138	188.056	10.82	-3.4E-01	-3.1E-01
A_0046	N-Acetylmethionine	448580	HMDB0011745	190.055	6.89	-9.1E-01	1.6E-01
A_0048	XA0019			191.019	7.05	9.1E-01	1.5E-01
A_0049	Citric acid	311	HMDB0000094	191.020	17.85	-7.4E-01	-4.4E-01
A_0050	Quinic acid	6508	HMDB0003072	191.065	6.55	-3.0E-02	-1.4E-01
A_0051	N-(o-Toluoyl)glycine	91637	HMDB0011723	192.065	6.91	6.1E-01	-7.2E-01
A_0052	Phenaceturic acid	68144	HMDB0000821	192.066	6.97	-4.2E-01	-4.9E-01
A_0053	Galacturonic acid-1 Glucuronic acid-1	439215 94715	HMDB0002545 HMDB0000127	193.035	7.01	-4.7E-01	-5.2E-01
A_0054	Galacturonic acid-2 Glucuronic acid-2	439215 94715	HMDB0002545 HMDB0000127	193.036	6.87	4.6E-01	-2.5E-02
A_0055	Gluconic acid	10690	HMDB0000625	195.050	6.96	8.8E-01	3.0E-01
A_0057	Lauric acid	3893	HMDB0000638	199.171	6.53	7.6E-01	4.5E-01
A_0058	Mucic acid	3037582	HMDB0000639	209.029	11.41	1.4E-01	-2.1E-01
A_0059	3-Indoxylsulfuric acid	10258	HMDB0000682	212.001	8.01	-9.7E-01	1.7E-01
A_0060	Pantothenic acid	6613	HMDB0000210	218.102	6.52	6.0E-01	-1.8E-01
A_0061	Ethyl glucuronide	18392195	HMDB0010325	221.066	6.61	4.7E-01	-8.5E-01
A_0062	Myristoleic acid	5281119	HMDB0002000	225.185	6.38	7.5E-01	6.0E-01
A_0063	Myristic acid	11005	HMDB0000806	227.202	6.36	2.9E-02	7.1E-01
A_0064	Ribulose 5-phosphate	439184	HMDB0000618	229.012	9.14	-9.3E-01	-7.3E-02
A_0065	Ribose 5-phosphate	439167	HMDB0001548	229.012	8.80	-8.2E-01	-7.7E-03
A_0066	XA0033			242.080	6.47	9.5E-02	-2.6E-01
A_0067	Ascorbate 2-sulfate	54676864		254.982	11.59	-7.8E-01	4.0E-01
A_0068	XA0035			254.983	11.08	-9.0E-01	1.7E-01
A_0069	Glucosamine 6-phosphate	440997	HMDB0001254	258.038	7.49	-5.3E-01	-3.0E-01
A_0070	myo-Inositol 2-phosphate	160886		259.022	8.80	-5.4E-01	3.3E-01
A_0071	Glucose 6-phosphate	5958	HMDB0001401	259.023	8.26	-5.4E-01	-3.2E-01

ID	Name	PubChem	HMDB	Mass	RT	Val1	Val2
A_0072	*myo*-Inositol 1-phosphate *myo*-Inositol 3-phosphate	107737 440194	HMDB0000213 HMDB0006814	259.023	8.61	4.8E-01	4.6E-01
A_0073	Glucose 1-phosphate	65533	HMDB0001586	259.023	8.48	-8.3E-01	-2.1E-01
A_0074	Fructose 6-phosphate	603	HMDB0000124	259.023	8.34	-4.7E-01	-4.1E-01
A_0075	Sorbitol 6-phosphate	152306	HMDB0005831	261.037	8.36	1.5E-01	4.8E-01
A_0076	2,3-Diphosphoglyceric acid	186004	HMDB0001294	264.953	14.19	8.0E-01	2.1E-01
A_0077	6-Phosphogluconic acid	91493	HMDB0001316	275.019	11.83	-9.7E-01	-9.1E-02
A_0078	Xanthosine	64959	HMDB0000299	283.070	6.47	-2.9E-01	8.3E-01
A_0079	Sedoheptulose 7-phosphate	165007	HMDB0001068	289.034	8.08	2.9E-01	-4.4E-01
A_0080	*N*-Acetylglucosamine 1-phosphate	440272	HMDB0001367	300.047	8.03	7.2E-01	2.6E-01
A_0081	*N*-Acetylglucosamine 6-phosphate	440996	HMDB0001062	300.048	7.72	-3.8E-01	-4.0E-01
A_0082	*N*-Acetylneuraminic acid	439197	HMDB0000230	308.100	6.14	3.4E-01	2.8E-01
A_0083	Ribulose 1,5-diphosphate	123658		308.979	12.45	5.6E-01	3.6E-01
A_0085	CMP	6131	HMDB0000095	322.043	8.04	3.5E-01	-1.6E-01
A_0086	UMP	6030	HMDB0000288	323.030	8.18	-7.5E-03	9.1E-01
A_0087	*N*-Glycolylneuraminic acid	440001	HMDB0000833	324.095	6.12	-7.9E-01	1.1E-01
A_0089	5-Aminoimidazole-4-carboxamide ribotide	65110	HMDB0001517	337.055	7.93	6.9E-01	3.9E-01
A_0090	Ascorbate 2-glucoside	54693473		337.075	6.09	-9.3E-01	3.6E-02
A_0091	Fructose 1,6-diphosphate	172313	HMDB0001058	338.989	11.73	-9.8E-01	-7.0E-02
A_0093	AMP	6083	HMDB0000045	346.056	7.78	-2.9E-01	9.0E-01
A_0094	3'-AMP	41211	HMDB0003540	346.058	8.16	-9.3E-01	-1.1E-01
A_0095	IMP	8582	HMDB0000175	347.042	7.98	-1.2E-01	8.5E-01
A_0096	GMP	6804	HMDB0001397	362.052	7.68	-1.9E-01	9.2E-01
A_0097	XA0055			368.999	11.56	-7.7E-01	-2.8E-01
A_0098	CoA_divalent	87642	HMDB0001423	382.549	8.82	7.6E-01	5.6E-01
A_0099	PRPP	7339	HMDB0000280	388.945	13.08	5.1E-01	1.7E-01
A_0100	FAD_divalent	643975	HMDB0001248	391.571	6.67	3.1E-01	6.6E-01
A_0103	UDP	6031	HMDB0000295	402.991	9.57	3.1E-01	-2.2E-01
A_0105	Cholic acid	221493	HMDB0000619	407.279	5.87	-8.1E-01	2.6E-01
A_0106	Thiamine diphosphate	1132	HMDB0001372	423.031	6.73	5.5E-01	-2.8E-01
A_0107	3-Methylcrotonyl CoA_divalent	9549326	HMDB0001493	423.570	8.60	-2.7E-01	3.8E-01
A_0109	ADP	6022	HMDB0001341	426.025	9.01	6.4E-01	6.6E-01
A_0110	GDP	8977	HMDB0001201	442.015	8.81	2.2E-01	8.5E-01
A_0111	XA0065			445.054	5.92	2.4E-01	7.7E-01
A_0112	Adenylosuccinic acid	447145	HMDB0000536	462.069	11.15	-9.6E-01	2.2E-01
A_0117	CDP-choline	13804	HMDB0001413	487.100	5.80	4.7E-01	7.3E-01
A_0119	ATP	5957	HMDB0000538	505.987	9.64	9.2E-01	-3.4E-01
A_0120	ITP	8583	HMDB0000189	506.972	9.65	5.5E-01	7.3E-01
A_0121	GTP	6830	HMDB0001273	521.976	9.42	9.2E-01	-3.6E-01
A_0122	ADP-ribose	445794	HMDB0001178	558.068	7.18	-8.8E-01	2.8E-01
A_0123	UDP-galactose UDP-glucose	23724458 8629	HMDB0000302 HMDB0000286	565.044	7.28	-9.7E-01	9.7E-02
A_0124	UDP-glucuronic acid	17473	HMDB0000935	579.030	9.15	8.0E-01	1.1E-01
A_0125	GDP-fucose ADP-glucose	10918995 16500	HMDB0001095 HMDB0006557	588.075	7.02	-4.5E-01	5.0E-01
A_0126	UDP-*N*-acetylgalactosamine UDP-*N*-acetylglucosamine	23724461 445675	HMDB0000304 HMDB0000290	606.069	7.13	-9.6E-01	-2.7E-02
A_0127	CMP-*N*-acetylneuraminate	448209	HMDB0001176	613.143	7.03	-5.7E-01	-5.5E-01
A_0128	NAD+	5893	HMDB0000902	662.105	5.59	9.6E-01	2.7E-01
A_0129	NADH+	439153	HMDB0001487	664.111	6.91	9.1E-01	-1.3E-01
A_0130	NADP+	5886	HMDB0000217	742.067	7.85	8.8E-01	1.8E-01
C_0001	Trimethylamine	1146	HMDB0000906	60.081	4.82	-8.7E-01	-3.0E-01
C_0002	Urea	1176	HMDB0000294	61.040	17.31	-7.4E-02	-3.6E-01
C_0003	Ethanolamine	700	HMDB0000149	62.061	5.20	9.0E-01	2.5E-01
C_0004	XC0001			72.081	5.21	-9.9E-01	-7.8E-02
C_0005	Aminoacetone	215	HMDB0002134	74.060	5.60	-2.0E-01	1.9E-02
C_0006	Gly	750	HMDB0000123	76.040	6.80	-9.3E-01	-2.8E-03
C_0007	Isopropanolamine	4	HMDB0012136	76.075	5.71	-4.8E-01	-5.2E-03
C_0008	Trimethylamine *N*-oxide	1145	HMDB0000925	76.076	5.40	-9.3E-01	5.4E-02
C_0009	Putrescine	1045	HMDB0001414	89.108	3.87	-3.3E-02	6.2E-01
C_0010	β-Ala	239	HMDB0000056	90.055	5.98	9.6E-01	1.2E-01
C_0011	Sarcosine	1088	HMDB0000271	90.055	7.75	5.8E-01	3.5E-01
C_0012	Ala	602	HMDB0000161,HMDB0001310	90.055	7.35	-9.5E-01	-1.4E-01
C_0013	Dimethylaminoethanol	7902	HMDB0032231	90.092	5.64	-2.3E-01	2.2E-01
C_0014	Glycerol	753	HMDB0000131	93.055	18.05	5.5E-01	-4.1E-01
C_0015	Phenol	996	HMDB0000228	95.048	4.41	5.3E-01	-5.8E-01
C_0016	Homoserinelactone	73509		102.055	5.77	3.0E-01	9.1E-02
C_0017	Azetidine 2-carboxylic acid	16486		102.055	9.40	-4.8E-01	-5.2E-03
C_0018	Hexylamine	8102		102.127	6.18	-8.0E-01	3.6E-01
C_0019	3-Aminoisobutyric acid	64956	HMDB0003911	104.071	6.40	-9.3E-01	-2.5E-01
C_0020	GABA	119	HMDB0000112	104.071	6.27	-8.6E-01	4.1E-01

ID	Name	CID	HMDB	Mass	RT	V1	V2
C_0021	3-Aminobutyric acid	10932		104.071	6.48	7.7E-01	-5.7E-01
C_0022	2-Aminoisobutyric acid 2-Aminobutyric acid	6119 6657	HMDB0001906 HMDB0000452	104.071	7.84	-5.0E-01	3.0E-01
C_0023	*N*,*N*-Dimethylglycine	673	HMDB0000092	104.071	8.91	2.8E-01	3.7E-01
C_0024	Choline	305	HMDB0000097	104.107	5.58	8.1E-01	2.1E-01
C_0025	2,3-Diaminopropionic acid	364	HMDB0002006	105.067	5.86	-7.9E-01	-2.3E-01
C_0026	Ser	617	HMDB0000187,HMDB0003406	106.050	8.17	-8.7E-01	-2.8E-01
C_0027	Diethanolamine	8113	HMDB0004437	106.087	6.23	6.0E-02	2.8E-01
C_0028	Hypotaurine	107812	HMDB0000965	110.027	14.56	-5.1E-01	-7.5E-01
C_0029	Cytosine	597	HMDB0000630	112.052	5.92	-9.9E-01	2.3E-02
C_0030	Histamine	774	HMDB0000870	112.088	3.94	4.2E-01	5.0E-01
C_0031	Uracil	1174	HMDB0000300	113.035	18.10	3.9E-01	-7.4E-01
C_0032	Creatinine	588	HMDB0000562	114.067	5.94	3.9E-01	-1.4E-01
C_0033	3-Amino-2-piperidone	5200225	HMDB0000323	115.086	6.20	-3.2E-01	4.4E-01
C_0034	Pro	614	HMDB0000162,HMDB0003411	116.071	8.79	1.4E-01	3.4E-01
C_0035	Guanidoacetic acid	763	HMDB0000128	118.062	6.72	-5.5E-01	5.8E-01
C_0036	Val	1182	HMDB0000883	118.087	8.13	3.0E-01	9.1E-01
C_0037	Betaine	247	HMDB0000043	118.087	9.17	8.0E-01	-4.8E-01
C_0038	5-Aminovaleric acid	138	HMDB0003355	118.087	6.52	-9.6E-01	6.5E-02
C_0039	2,4-Diaminobutyric acid	134490	HMDB0006284	119.082	5.65	-9.4E-01	-9.5E-02
C_0040	4-Amino-3-hydroxybutyric acid	2149		120.064	6.61	-5.5E-01	-2.1E-01
C_0041	Thr	6288	HMDB0000167	120.066	8.57	-7.9E-01	1.2E-01
C_0042	Homoserine	12647	HMDB0000719	120.066	8.22	-8.9E-01	-1.5E-01
C_0043	2-Methylserine	439656		120.067	8.45	-7.6E-01	-3.6E-01
C_0044	Betaine aldehyde_+H$_2$O	249	HMDB0001252	120.103	6.06	8.2E-01	-1.4E-01
C_0045	Anserine_divalent	112072	HMDB0000194	121.069	5.56	-4.6E-01	3.5E-01
C_0046	Cys	594	HMDB0000574,HMDB0003417	122.028	9.22	-9.6E-01	2.7E-01
C_0047	2-Amino-2-(hydroxymethyl)-1,3-propanediol	6503		122.082	6.74	-6.6E-01	-1.0E-01
C_0048	Nicotinamide	936	HMDB0001406	123.056	6.04	-6.4E-01	-3.8E-01
C_0049	Nicotinic acid	938	HMDB0001488	124.040	8.19	-3.1E-01	-6.8E-01
C_0050	Picolinic acid	1018	HMDB0002243	124.040	15.28	3.3E-01	-6.5E-01
C_0051	Taurine	1123	HMDB0000251	126.022	18.03	8.9E-01	2.2E-01
C_0052	1-Methylhistamine	3614	HMDB0000898	126.103	4.04	3.7E-01	4.9E-01
C_0053	3-Hydroxy-2-methyl-4-pyrone	8369	HMDB0030776	127.038	18.07	-9.9E-01	-6.0E-02
C_0055	Imidazole-4-acetic acid	96215	HMDB0002024	127.051	6.54	-1.5E-01	-1.6E-01
C_0056	XC0016			129.067	7.13	-7.1E-01	3.2E-01
C_0057	4-Oxopyrrolidine-2-carboxylic acid	107541		130.050	8.92	6.1E-01	3.0E-02
C_0058	Pipecolic acid	439227	HMDB0000070,HMDB0000716,HMDB0005960	130.087	8.34	-5.8E-01	-5.8E-01
C_0059	*trans*-Glutaconic acid	5280498	HMDB0000620	131.034	18.78	-7.2E-01	2.8E-01
C_0060	*cis*-4-Hydroxyproline	440014	HMDB0006055	132.066	8.97	5.8E-01	-5.8E-01
C_0061	Hydroxyproline	5810	HMDB0000725	132.067	9.79	-8.9E-01	-1.6E-01
C_0062	3-Guanidinopropionic acid	67701		132.077	6.53	-9.0E-01	-1.9E-01
C_0063	Creatine	586	HMDB0000064	132.078	7.20	-1.8E-02	-5.5E-02
C_0064	Ile	791	HMDB0000172	132.102	8.28	7.4E-02	9.5E-01
C_0065	Leu	857	HMDB0000687	132.102	8.37	1.6E-01	9.4E-01
C_0066	Asn	236	HMDB0000168,HMDB0033780	133.061	8.58	-8.0E-01	5.4E-01
C_0067	Gly-Gly	11163	HMDB0011733	133.062	6.80	6.6E-01	7.0E-01
C_0068	Ornithine	389	HMDB0000214,HMDB0003374	133.098	5.55	6.6E-01	-5.2E-01
C_0069	Thiaproline	9934		134.028	11.38	4.0E-01	6.9E-01
C_0070	Asp	424	HMDB0000191,HMDB0006483	134.045	9.47	-8.9E-01	-7.9E-02
C_0071	Adenine	190	HMDB0000034	136.063	6.22	2.6E-01	-8.8E-01
C_0072	Hypoxanthine	790	HMDB0000157	137.047	9.27	6.8E-01	-6.7E-01
C_0073	1-Methylnicotinamide	457	HMDB0000699	137.072	5.99	-8.1E-01	4.9E-01
C_0074	Trigonelline	5570	HMDB0000875	138.056	8.53	-5.7E-01	-2.3E-01
C_0075	Anthranilic acid	227	HMDB0001123	138.056	8.87	6.7E-01	7.2E-02
C_0077	γ-Glu-Lys_divalent	65254	HMDB0029154	138.581	6.99	-1.5E-01	6.8E-02
C_0078	Urocanic acid	736715	HMDB0000301	139.051	6.76	-7.5E-02	5.9E-01
C_0079	1-Methyl-4-imidazoleacetic acid	75810	HMDB0002820	141.066	6.71	-8.5E-02	-9.0E-01
C_0080	1*H*-Imidazole-4-propionic acid	10105257		141.067	6.61	-7.4E-01	-9.0E-02
C_0081	Ectoine	126041		143.082	7.65	5.4E-02	-3.6E-01
C_0082	XC0029 Stachydrine	0 115244	HMDB0004827	144.102	9.32	3.8E-01	-4.6E-02
C_0083	4-Guanidinobutyric acid	500	HMDB0003464	146.093	6.75	-7.2E-01	7.1E-02
C_0084	γ-Butyrobetaine	134	HMDB0001161	146.118	6.60	-9.4E-01	-6.9E-02
C_0085	Spermidine	1102	HMDB0001257	146.166	3.72	-4.7E-01	-2.5E-01
C_0086	Gln	738	HMDB0000641,HMDB0003423	147.077	8.76	-8.9E-01	3.5E-01
C_0087	Lys	866	HMDB0000182,HMDB0003405	147.113	5.60	-2.8E-01	5.7E-02
C_0088	Isoglutamic acid	73064		148.061	7.45	8.4E-01	-2.6E-01
C_0089	Glu	611	HMDB0000148,HMDB0003339	148.061	8.92	7.5E-01	-1.1E-01
C_0090	*threo*-β-Methylaspartic acid	440064		148.062	10.05	-1.1E-01	1.7E-02
C_0091	Met	876	HMDB0000696	150.059	8.73	7.5E-01	1.2E-01

ID	Name	CID	HMDB	Mass	RT	Val1	Val2
C_0092	Guanine	764	HMDB0000132	152.059	6.79	7.8E-01	-4.6E-01
C_0093	Xanthine	1188	HMDB0000292	153.042	16.04	9.4E-01	2.0E-01
C_0094	N^1-Methyl-4-pyridone-5-carboxamide	440810	HMDB0004194	153.066	15.08	2.6E-01	6.2E-01
C_0095	4-(β-Acetylaminoethyl)imidazole	69602		154.097	6.85	1.4E-01	3.8E-01
C_0096	His	773	HMDB0000177	156.078	5.95	-9.3E-01	6.5E-02
C_0097	Imidazolelactic acid	793		157.061	7.18	-5.1E-01	2.5E-01
C_0098	XC0145 / Ala-Ala	15331 / 5460362	HMDB0003459	161.093	7.52	-6.4E-01	5.4E-01
C_0099	Tryptamine	1150	HMDB0000303	161.106	6.76	4.0E-01	-8.0E-01
C_0100	N^6-Methyllysine	164795	HMDB0002038	161.129	5.79	-9.4E-01	-1.0E-01
C_0101	O-Acetylhomoserine / 2-Aminoadipic acid	439389 / 92136	HMDB0000510	162.077	8.92	1.6E-01	2.1E-01
C_0102	Carnitine	85	HMDB0000062	162.113	6.92	-1.0E-01	-9.6E-01
C_0103	5-Hydroxylysine	3032849	HMDB0000450	163.109	5.83	1.4E-01	5.4E-01
C_0104	Pterin	73000	HMDB0000802	164.057	8.49	8.6E-01	1.5E-01
C_0105	Phe	994	HMDB0000159	166.087	9.00	2.4E-02	7.7E-01
C_0106	Tyr-Arg_divalent	123804		169.595	6.27	5.1E-01	4.8E-01
C_0107	1-Methylhistidine / 3-Methylhistidine	92105 / 64969	HMDB0000001 / HMDB0000479	170.094	6.12	-7.3E-01	-1.1E-01
C_0108	XC0147	4173		172.072	7.85	4.9E-01	5.5E-01
C_0109	XC0040			174.088	9.79	-1.2E-01	-7.8E-01
C_0110	N^5-Ethylglutamine	439378		175.109	9.24	-7.6E-01	-8.6E-02
C_0111	N-Acetylornithine	439232	HMDB0003357	175.109	7.73	-1.4E-01	4.9E-01
C_0112	Arg	6322	HMDB0000517,HMDB0003416	175.120	5.81	-9.7E-01	-4.4E-02
C_0113	Guanidinosuccinic acid	439918	HMDB0003157	176.068	8.23	-9.7E-01	1.1E-01
C_0114	Citrulline	9750	HMDB0000904	176.104	8.99	8.8E-01	-3.6E-01
C_0115	Serotonin	5202	HMDB0000259	177.103	7.13	3.9E-01	-2.0E-01
C_0116	Gluconolactone	7027	HMDB0000150	179.056	18.76	8.8E-01	3.2E-01
C_0117	Glucosamine	439213	HMDB0001514	180.088	7.54	-9.2E-01	-3.2E-01
C_0118	Tyr	1153	HMDB0000158	182.082	9.22	-5.9E-01	6.5E-01
C_0119	Phosphorylcholine	1014	HMDB0001565	184.074	16.66	-4.3E-01	-3.6E-01
C_0120	N^1-Acetylspermidine	496	HMDB0001276	188.177	5.16	-4.1E-01	2.4E-01
C_0121	Gly-Leu			189.124	7.83	3.9E-01	7.3E-01
C_0122	N-Acetyllysine	92907	HMDB0000446	189.125	7.93	-2.6E-01	4.1E-01
C_0123	N^6-Acetyllysine	92832	HMDB0000206	189.125	9.29	5.0E-01	-2.3E-01
C_0124	N_ω-Methylarginine	132862		189.136	6.07	-3.5E-01	-4.0E-01
C_0125	N^6,N^6,N^6-Trimethyllysine	440120	HMDB0001325	189.159	5.86	8.3E-01	1.6E-01
C_0126	Homocitrulline	65072	HMDB0000679	190.120	9.08	-8.8E-01	2.4E-01
C_0127	Gly-Asp	97363		191.067	8.04	-4.4E-01	8.0E-01
C_0128	2,6-Diaminopimelic acid	439283	HMDB0001370	191.103	7.24	-3.7E-01	-5.7E-01
C_0129	N-Acetylhistidine	75619		198.089	7.97	-7.3E-01	1.3E-01
C_0130	11-Aminoundecanoic acid	17083		202.182	7.81	4.9E-01	7.7E-01
C_0131	SDMA	169148	HMDB0003334	203.151	6.35	8.1E-01	-4.0E-01
C_0132	ADMA	123831	HMDB0001539	203.151	6.24	2.0E-01	-9.2E-01
C_0133	Spermine	1103	HMDB0001256	203.225	3.67	9.7E-01	-1.4E-01
C_0134	O-Acetylcarnitine	439756	HMDB0000201	204.124	7.33	-9.3E-02	-7.5E-01
C_0135	γ-Glu-Gly	165527	HMDB0011667	205.083	9.81	-9.6E-01	-1.4E-01
C_0136	Trp	1148	HMDB0000929	205.098	8.95	-7.5E-01	4.7E-01
C_0137	Carboxymethyllysine	123800		205.120	7.52	9.3E-01	1.5E-01
C_0138	Kynurenine	846	HMDB0000684	209.094	8.17	1.5E-01	7.9E-02
C_0139	Propionylcarnitine / XC0061	1888240	HMDB0000824	218.140	7.57	4.4E-01	-6.0E-01
C_0140	β-Ala-Lys	440638		218.151	5.54	-8.2E-01	4.5E-01
C_0141	XC0065			221.093	10.63	-6.3E-01	-4.3E-01
C_0142	N-Acetylglucosylamine	439454	HMDB0001104	221.114	8.05	8.7E-01	-2.6E-01
C_0143	N-Acetylgalactosamine / N-Acetylglucosamine / N-Acetylmannosamine	35717 / 439174 / 439281	HMDB0000853 / HMDB0000215 / HMDB0001129	222.099	18.09	1.4E-01	-6.7E-01
C_0144	Carnosine	439224	HMDB0000033	227.115	5.51	3.3E-01	-4.1E-01
C_0145	Ergothioneine	3037043	HMDB0003045	230.097	14.04	7.8E-01	-4.5E-01
C_0146	Butyrylcarnitine	439829	HMDB0002013	232.156	7.77	-4.4E-01	3.9E-01
C_0147	Ser-Glu			235.094	8.43	-7.1E-01	4.6E-01
C_0148	γ-Glu-Ser	22844748	HMDB0029158	235.094	10.25	-7.8E-01	1.3E-01
C_0149	Thr-Asp	3280446		235.095	8.61	-6.4E-01	5.1E-01
C_0150	7,8-Dihydrobiopterin	119055	HMDB0000038	240.110	8.96	2.8E-01	-5.1E-02
C_0151	Thymidine	5789	HMDB0000273	243.098	18.18	-7.1E-01	1.7E-01
C_0152	Cytidine	6175	HMDB0000089	244.095	7.86	6.8E-01	-7.0E-01
C_0153	Uridine	6029	HMDB0000296	245.078	18.11	-9.3E-01	-2.6E-01
C_0154	Isovalerylcarnitine	6426851	HMDB0000688	246.170	7.87	8.4E-01	2.8E-01
C_0155	γ-Glu-Val	7015683	HMDB0011172	247.131	10.33	-1.9E-02	-6.0E-01
C_0156	Malonylcarnitine	22833583	HMDB0002095	248.114	8.28	5.7E-01	3.0E-01

C_0157	Pyridoxamine 5'-phosphate	1053	HMDB0001555	249.065	8.51	6.4E-01	-8.9E-02
C_0158	γ-Glu-Thr	53861142	HMDB0029159	249.110	10.34	-1.8E-01	-8.0E-01
C_0159	γ-Glu-Cys	123938	HMDB0001049	251.071	10.43	-7.0E-01	5.7E-01
C_0160	XC0153	4725		254.123	8.45	-5.5E-01	8.1E-01
C_0161	XC0089			255.100	7.72	9.2E-01	-3.2E-01
C_0162	XC0154	3182		255.110	18.12	-9.4E-01	-2.7E-02
C_0163	Glycerophosphocholine	439285	HMDB0000086	258.112	17.68	-9.2E-01	-4.1E-02
C_0164	γ-Glu-Ile γ-Glu-Leu	22885096 151023	HMDB0011170 HMDB0011171	261.146	10.49	-1.1E-01	-5.1E-02
C_0165	γ-Glu-Asn	131801686	HMDB0029144	262.103	10.37	4.4E-01	5.6E-02
C_0166	γ-Glu-Ornitine	189156	HMDB0002248	262.141	6.93	3.2E-01	8.2E-01
C_0167	γ-Glu-Asp	161197	HMDB0030419	263.087	10.57	7.1E-02	9.0E-01
C_0168	Thiamine	1130	HMDB0000235	265.113	5.36	-9.6E-01	-1.6E-01
C_0169	Adenosine	60961	HMDB0000050	268.105	8.03	6.6E-01	-4.0E-01
C_0170	Inosine	6021	HMDB0000195	269.089	16.01	2.5E-02	-9.3E-01
C_0171	γ-Glu-Glu	92865	HMDB0011737	277.105	10.66	2.7E-01	-7.9E-01
C_0172	Glu-Glu	439500		277.106	8.85	-2.5E-01	9.3E-01
C_0173	Saccharopine	160556	HMDB0000279	277.141	8.74	8.7E-01	3.1E-01
C_0174	1-Methyladenosine	27476	HMDB0003331	282.122	8.08	5.7E-01	4.4E-01
C_0175	Guanosine	6802	HMDB0000133	284.101	10.31	6.0E-01	-7.7E-01
C_0176	His-Glu	7010583		285.121	6.16	-7.8E-01	1.5E-01
C_0177	Ophthalmic acid	7018721	HMDB0005765	290.135	10.73	-7.1E-01	-3.4E-01
C_0178	Argininosuccinic acid	16950	HMDB0000052	291.131	7.69	-9.8E-01	1.1E-01
C_0179	γ-Glu-Phe	111299	HMDB0000594	295.130	10.59	-3.0E-02	-6.3E-01
C_0180	5'-Deoxy-5'-methylthioadenosine	439176	HMDB0001173	298.098	8.18	-5.0E-01	-2.4E-01
C_0181	Arg-Glu			304.163	6.11	-7.1E-01	3.9E-01
C_0182	Glutathione (GSSG)_divalent	65359	HMDB0003337	307.085	9.91	-4.2E-01	-5.2E-01
C_0183	Glutathione (GSH)	124886	HMDB0000125	308.093	10.75	-9.6E-01	-1.0E-01
C_0184	XC0126			310.114	12.18	5.4E-01	-2.9E-01
C_0185	Tyr-Glu			311.125	9.03	-5.8E-01	3.7E-01
C_0186	S-Methylglutathione	115260		322.108	10.86	-9.1E-01	-4.9E-02
C_0187	XC0132			325.162	7.06	3.3E-01	9.8E-02
C_0188	NMN	14180	HMDB0000229	335.066	16.77	9.6E-01	-4.2E-02
C_0189	Thiamine phosphate	1131	HMDB0002666	345.080	8.67	6.9E-01	3.9E-01
C_0190	XC0137			350.103	10.98	2.4E-01	-4.0E-01
C_0191	S-Lactoylglutathione	440018	HMDB0001066	380.114	11.20	7.7E-01	-4.5E-01
C_0192	S-Adenosylhomocysteine	439155	HMDB0000939	385.130	7.13	8.4E-01	4.5E-01
C_0193	S-Adenosylmethionine	34755	HMDB0001185	399.146	5.81	-9.1E-01	9.7E-02
C_0194	Tetrahydrofolic acid	135444742	HMDB0001846	446.181	9.65	-1.3E-01	-4.3E-01
C_0195	5-Methyltetrahydrofolic acid	444412	HMDB0001396	460.196	9.63	-5.0E-01	-1.8E-01

MT, migration time; PC, principal component; RT, retention time

Supplementary Table S3. Results of comparative analyses

| | | | | Concentration (nmol/g) | | | | | | | | | | Comparative Analysis | |
| | | | | Group I | | | Group C | | | Group I | | Group C | | Group I vs Group C | |
ID	Metabolite	PubChem CID	HMDB ID	I1	I2	I3	C5	C6	C7	Mean	S.D.	Mean	S.D.	Ratio †	p-value ‡
A_0007	2-Hydroxybutyric acid	440864	HMDB0000008	23	N.D.	42	68	74	27	32	14	56	26	0.6	0.267
A_0021	2-Oxoglutaric acid	51	HMDB0000208	N.D.	N.D.	N.D.	N.D.	N.D.	N.D.	N.A.	N.A.	N.A.	N.A.	N.A.	N.A.
A_0009	2-Oxoisovaleric acid	49	HMDB0000019	N.D.	N.D.	N.D.	N.D.	N.D.	N.D.	N.A.	N.A.	N.A.	N.A.	N.A.	N.A.
A_0041	2-Phosphoglyceric acid	439278	HMDB0003391	N.D.	N.D.	N.D.	N.D.	N.D.	N.D.	N.A.	N.A.	N.A.	N.A.	N.A.	N.A.
A_0006	3-Hydroxybutyric acid	441	HMDB0000011,HMDB0003357,HMDB0000442	240	322	413	727	1,008	499	325	87	744	255	0.4	0.092
A_0040	3-Phosphoglyceric acid	439183	HMDB0000807	N.D.	N.D.	28	17	28	28	28	N.A.	25	6.3	1.1	N.A.
A_0077	6-Phosphogluconic acid	91493	HMDB0001316	110	99	81	37	48	44	97	15	43	5.6	2.2	0.015 *
A_0104	Acetyl CoA_divalent	444493		N.D.	N.D.	N.D.	N.D.	N.D.	N.D.	N.A.	N.A.	N.A.	N.A.	N.A.	N.A.
C_0071	Adenine	190	HMDB0000034	8.1	7.1	6.9	7.2	6.8	11	7.4	0.6	8.3	2.2	0.9	0.537
C_0169	Adenosine	60961	HMDB0000050	69	49	47	63	83	73	55	12	73	10	0.8	0.123
A_0109	ADP	6022	HMDB0001341	106	99	115	141	146	99	107	7.9	129	26	0.8	0.278
C_0012	Ala	602	HMDB0000161,HMDB0001310	2,722	2,240	2,372	1,435	1,167	1,651	2,445	249	1,418	243	1.7	0.007 **
A_0093	AMP	6083	HMDB0000045	788	748	889	894	791	331	808	72	672	299	1.2	0.516
C_0075	Anthranilic acid	227	HMDB0001123	N.D.	N.D.	0.4	0.3	0.3	0.4	0.4	N.A.	0.3	0.07	1.2	N.A.
C_0112	Arg	6322	HMDB0000517,HMDB0003416	8.7	7.6	5.8	3.5	2.8	2.9	7.4	1.4	3.1	0.4	2.4	0.030 *
C_0086	Asn	236	HMDB0000168,HMDB0003780	230	215	246	200	168	142	230	16	170	29	1.4	0.090
C_0070	Asp	424	HMDB0000191,HMDB0006483	576	592	519	398	473	413	562	38	417	54	1.3	0.023 *
A_0119	ATP	5957	HMDB0000538	15	18	16	28	37	40	16	1.6	35	6.5	0.5	0.031 *
C_0037	Betaine	247	HMDB0000043	1,077	948	1,092	1,195	1,520	1,624	1,039	79	1,433	247	0.7	0.098
A_0044	Betaine aldehyde_+H2O	249		52	53	64	64	99	84	56	7.1	82	17	0.7	0.107
A_0088	cAMP	6076	HMDB0000058	N.D.	N.D.	N.D.	N.D.	N.D.	N.D.	N.A.	N.A.	N.A.	N.A.	N.A.	N.A.
C_0144	Carnosine	439224	HMDB0000033	0.4	0.8	0.6	0.8	0.5	1.0	0.6	0.2	0.8	0.3	0.8	0.451
A_0102	CDP	6132	HMDB0001546	N.D.	N.D.	N.D.	N.D.	N.D.	N.D.	N.A.	N.A.	N.A.	N.A.	N.A.	N.A.
A_0092	cGMP	24316	HMDB0001314	N.D.	N.D.	N.D.	N.D.	N.D.	N.D.	N.A.	N.A.	N.A.	N.A.	N.A.	N.A.
C_0024	Choline	305	HMDB0000097	398	417	488	581	857	552	434	47	664	168	0.7	0.134
A_0034	cis-Aconitic acid	643757	HMDB0000072	N.D.	N.D.	N.D.	N.D.	N.D.	N.D.	N.A.	N.A.	N.A.	N.A.	N.A.	N.A.
A_0049	Citric acid	311	HMDB0000094	187	225	182	137	148	187	198	24	157	26	1.3	0.118
C_0114	Citrulline	9750	HMDB0000904	33	30	34	36	40	41	32	1.8	39	2.7	0.8	0.028 *
A_0085	CMP	6131	HMDB0000095	78	60	64	70	78	69	68	9.4	73	4.8	0.9	0.474
A_0098	CoA_divalent	87642		105	98	130	142	143	117	111	17	134	15	0.8	0.147
C_0063	Creatine	586	HMDB0000064	193	165	244	211	152	230	201	40	198	41	1.0	0.935
C_0032	Creatinine	588	HMDB0000562	4.4	4.3	5.5	5.4	4.3	5.9	4.7	0.7	5.2	0.8	0.9	0.471
A_0115	CTP	6176	HMDB0000082	N.D.	N.D.	N.D.	N.D.	N.D.	N.D.	N.A.	N.A.	N.A.	N.A.	N.A.	N.A.
C_0046	Cys	594	HMDB0000574,HMDB0003417	8.3	7.8	7.5	3.8	2.6	1.4	7.9	0.4	2.6	1.2	3.0	0.011 *
C_0152	Cytidine	6175	HMDB0000089	6.8	4.4	4.9	6.6	8.2	11	5.4	1.2	8.8	2.5	0.6	0.125
C_0029	Cytosine	597	HMDB0000630	0.6	0.5	0.5	N.D.	N.D.	N.D.	0.5	0.08	N.A.	N.A.	1<	N.A.
A_0118	dATP	15993	HMDB0001532	N.D.	N.D.	N.D.	N.D.	N.D.	N.D.	N.A.	N.A.	N.A.	N.A.	N.A.	N.A.
A_0113	dCTP	65091	HMDB0000998	N.D.	N.D.	N.D.	N.D.	N.D.	N.D.	N.A.	N.A.	N.A.	N.A.	N.A.	N.A.
A_0029	Dihydroxyacetone phosphate	668	HMDB0001473	698	522	436	134	189	150	552	133	158	28	3.5	0.032 *
A_0101	dTDP	164628	HMDB0001274	N.D.	N.D.	N.D.	N.D.	N.D.	N.D.	N.A.	N.A.	N.A.	N.A.	N.A.	N.A.
A_0084	dTMP	9700	HMDB0001227	N.D.	N.D.	N.D.	N.D.	N.D.	N.D.	N.A.	N.A.	N.A.	N.A.	N.A.	N.A.
A_0114	dTTP	64968	HMDB0001342	N.D.	N.D.	N.D.	N.D.	N.D.	N.D.	N.A.	N.A.	N.A.	N.A.	N.A.	N.A.
A_0056	Erythrose 4-phosphate	122357	HMDB0001321	N.D.	N.D.	N.D.	N.D.	N.D.	N.D.	N.A.	N.A.	N.A.	N.A.	N.A.	N.A.
A_0091	Fructose 1,6-diphosphate	172313	HMDB0001058	412	313	257	30	20	42	327	78	31	11	11	0.021 *
A_0074	Fructose 6-phosphate	603	HMDB0000124	419	95	59	80	98	116	191	198	98	18	1.9	0.503
A_0008	Fumaric acid	444972	HMDB0000134	860	792	835	261	331	332	829	34	308	41	2.7	8.9E-05 ***
C_0020	GABA	119	HMDB0000112	38	41	49	24	27	18	43	5.5	23	4.5	1.9	0.009 **
A_0110	GDP	8977	HMDB0001201	21	21	26	24	25	20	23	2.8	23	2.3	1.0	0.875
C_0088	Gln	738	HMDB0000641,HMDB0003423	2,245	2,531	2,173	1,737	1,667	1,272	2,316	189	1,559	251	1.5	0.016 *
C_0089	Glu	611	HMDB0000148,HMDB0003339	1,662	1,528	1,422	1,735	2,099	1,743	1,537	120	1,859	208	0.8	0.098
A_0055	Gluconic acid	10690	HMDB0000625	629	483	602	1,014	1,045	734	571	78	931	172	0.6	0.051
A_0073	Glucose 1-phosphate	65533	HMDB0001586	222	106	72	25	20	25	133	79	23	3.2	5.7	0.136
A_0071	Glucose 6-phosphate	5958	HMDB0001401	1,726	234	126	149	163	155	695	894	156	6.9	4.5	0.405
C_0183	Glutathione (GSH)	124886	HMDB0000125	4,479	3,705	3,391	2,212	2,224	2,287	3,858	560	2,241	40	1.7	0.037 *
C_0182	Glutathione (GSSG)_divalent	65359		671	563	540	540	571	574	591	70	561	19	1.1	0.543
C_0008	Gly	750	HMDB0000123	1,980	1,679	1,781	1,396	1,404	1,388	1,814	153	1,396	7.7	1.3	0.042 *
A_0030	Glyceraldehyde 3-phosphate	729	HMDB0001112	36	N.D.	N.D.	N.D.	N.D.	N.D.	36	N.A.	N.A.	N.A.	1<	N.A.
A_0031	Glycerol 3-phosphate	439162	HMDB0000126	2,125	2,306	2,295	1,994	2,526	1,990	2,229	93	2,170	308	1.0	0.778
A_0002	Glycolic acid	757	HMDB0000115	N.D.	N.D.	N.D.	N.D.	N.D.	N.D.	N.A.	N.A.	N.A.	N.A.	N.A.	N.A.
A_0001	Glyoxylic acid	760	HMDB0000119	N.D.	N.D.	N.D.	N.D.	N.D.	N.D.	N.A.	N.A.	N.A.	N.A.	N.A.	N.A.
A_0096	GMP	6804	HMDB0001397	245	230	300	281	276	116	259	37	225	94	1.2	0.606
A_0121	GTP	6830	HMDB0001273	N.D.	N.D.	N.D.	7.1	12	14	N.A.	N.A.	11	3.8	<1	N.A.
C_0092	Guanine	764	HMDB0000132	2.9	2.7	3.3	3.3	5.3	5.6	3.0	0.3	4.7	1.2	0.6	0.130
C_0175	Guanosine	6802	HMDB0000133	57	47	46	51	66	82	50	6.3	66	16	0.8	0.199
C_0096	His	773	HMDB0000177	693	644	618	571	556	535	652	38	554	18	1.2	0.031 *
C_0042	Homoserine	12647	HMDB0000719	2.1	1.8	2.2	0.8	1.0	1.4	2.0	0.2	1.1	0.3	1.9	0.014 *
C_0061	Hydroxyproline	5810	HMDB0000725	22	19	24	9.6	10	16	22	2.3	12	3.3	1.8	0.017 *
C_0072	Hypoxanthine	790	HMDB0000157	821	721	792	821	972	1,175	778	52	989	178	0.8	0.168
C_0064	Ile	791	HMDB0000172	280	283	317	317	319	239	293	20	292	46	1.0	0.956
A_0095	IMP	8582	HMDB0000175	217	207	216	262	252	61	214	5.8	191	113	1.1	0.767
C_0170	Inosine	6021	HMDB0000195	2,078	1,789	1,834	1,708	1,856	2,241	1,901	155	1,935	275	1.0	0.862
A_0047	Isocitric acid	1198	HMDB0000193	N.D.	N.D.	N.D.	N.D.	N.D.	N.D.	N.A.	N.A.	N.A.	N.A.	N.A.	N.A.
A_0005	Lactic acid	612	HMDB0000190,HMDB0001311	14,946	14,349	17,523	5,675	3,948	5,925	15,606	1,687	5,183	1,077	3.0	0.002 **
C_0065	Leu	857	HMDB0000687	543	539	621	614	589	511	568	46	572	54	1.0	0.932
C_0087	Lys	866	HMDB0000182,HMDB0003405	1,130	1,035	1,249	1,171	902	1,152	1,138	107	1,075	150	1.1	0.588
A_0016	Malic acid	525	HMDB0000156,HMDB0007744	2,245	2,164	2,154	470	619	651	2,188	50	580	96	3.8	1.3E-04 ***
A_0108	Malonyl CoA_divalent	644066		N.D.	N.D.	N.D.	N.D.	N.D.	N.D.	N.A.	N.A.	N.A.	N.A.	N.A.	N.A.
C_0091	Met	876	HMDB0000696	202	176	207	222	212	214	195	16	216	5.3	0.9	0.144
C_0023	N,N-Dimethylglycine	673	HMDB0000092	43	29	47	46	41	39	40	9.6	42	3.7	0.9	0.683
A_0128	NAD+	5893	HMDB0000902	26	30	37	65	63	50	31	5.5	60	8.1	0.5	0.010 *
A_0130	NADP+	5886	HMDB0000217	16	13	11	32	30	21	13	2.5	28	5.7	0.5	0.031 *
C_0068	Ornithine	389	HMDB0000214,HMDB0003374	383	370	417	384	464	532	383	30	460	74	0.8	0.207
C_0105	Phe	994	HMDB0000159	301	288	334	314	310	288	307	24	304	14	1.0	0.851
A_0027	Phosphoenolpyruvic acid	1005	HMDB0000263	13	54	12	13	20	21	13	1.0	18	4.3	0.7	0.189
C_0034	Pro	614	HMDB0000162,HMDB0003411	306	259	343	305	309	299	303	42	304	5.4	1.0	0.953
A_0099	PRPP	7339	HMDB0000280	N.D.	N.D.	N.D.	N.D.	5.9	N.D.	N.A.	N.A.	5.9	N.A.	<1	N.A.
C_0039	Putrescine	1045	HMDB0001414	4.2	5.5	3.8	5.5	5.0	3.1	4.5	0.9	4.5	1.3	1.0	0.961
A_0003	Pyruvic acid	1060	HMDB0000243	N.D.	N.D.	N.D.	136	147	121	N.A.	N.A.	135	13	<1	N.A.
A_0065	Ribose 5-phosphate	439167	HMDB0001548	167	127	102	69	97	56	132	33	74	21	1.8	0.071
A_0064	Ribulose 5-phosphate	439184	HMDB0000618	707	667	661	574	613	590	678	25	592	20	1.1	0.011 *
C_0193	S-Adenosylmethionine	34755	HMDB0001185	56	56	64	29	37	35	58	4.7	34	4.1	1.7	0.003 **
C_0011	Sarcosine	1088	HMDB0000271	32	23	33	51	32	34	29	5.5	39	10	0.7	0.236
A_0079	Sedoheptulose 7-phosphate	165007	HMDB0001068	281	95	77	187	225	203	151	113	205	19	0.7	0.498
C_0026	Ser	617	HMDB0000187,HMDB0003406	735	694	719	578	630	657	716	21	622	40	1.2	0.037 *
C_0085	Spermidine	1102	HMDB0001257	36	41	36	31	31	30	34	7.9	31	0.5	1.1	0.511
C_0133	Spermine	1103	HMDB0001256	8.8	7.8	7.6	13	14	13	8.1	0.6	14	0.3	0.6	6.1E-04 ***
A_0010	Succinic acid	1110	HMDB0000254	535	721	724	482	623	475	660	108	526	84	1.3	0.170
C_0041	Thr	6288	HMDB0000167	493	469	514	437	453	451	492	22	447	8.5	1.1	0.059
C_0151	Thymidine	5789	HMDB0000273	3.0	2.2	2.4	N.D.	2.2	N.D.	2.5	0.4	2.2	N.A.	1.1	N.A.
C_0054	Thymine	1135	HMDB0000262	N.D.	N.D.	N.D.	N.D.	N.D.	N.D.	N.A.	N.A.	N.A.	N.A.	N.A.	N.A.
C_0136	Trp	1148	HMDB0000929	72	68	81	61	64	56	74	6.8	60	4.0	1.2	0.054
C_0118	Tyr	1153	HMDB0000158	254	223	281	237	217	184	253	29	212	27	1.2	0.153
C_0076	Tyramine	5610	HMDB0000306	N.D.	N.D.	N.D.	N.D.	N.D.	N.D.	N.A.	N.A.	N.A.	N.A.	N.A.	N.A.
A_0103	UDP	6031	HMDB0000295	6.9	6.9	5.7	7.7	6.4	7.1	6.5	0.7	7.0	0.6	0.9	0.392
A_0086	UMP	6030	HMDB0000288	131	118	141	175	145	57	130	11	126	61	1.0	0.913
C_0031	Uracil	1174	HMDB0000300	61	63	67	57	69	90	63	3.0	72	17	0.9	0.473
C_0153	Uridine	6029	HMDB0000296	460	368	384	192	221	283	404	49	232	46	1.7	0.012 *
A_0116	UTP	6133	HMDB0000285	N.D.	N.D.	N.D.	N.D.	N.D.	N.D.	N.A.	N.A.	N.A.	N.A.	N.A.	N.A.
C_0036	Val	1182	HMDB0000883	488	479	529	546	535	456	499	26	512	49	1.0	0.701
C_0010	β-Ala	239	HMDB0000056	123	175	205	279	279	275	167	42	278	2.6	0.6	0.044 *

N.A., Not Available; N.D., Not Detected
† The ratio of the detected mean values between the two groups.
‡ Welch's t-test (*p<0.05, **p<0.01, ***p<0.001)

参考文献

1. Barker, D.J.; Osmond, C. Infant mortality, childhood nutrition, and ischaemic heart disease in England and Wales. Lancet 1986, 1, 1077–1081.

2. Gluckman, P.D.; Hanson, M.A. Living with the past: Evolution, development, and patterns of disease. Science 2004, 305, 1733–1736.

3. De Boo, H.A.; Harding, J.E. The developmental origins of adult disease (Barker) hypothesis. Aust. N. Z. J. Obstet. Gynaecol. 2006, 46, 4–14.

4. Ministry of Health, Labor and Welfare in Japan. Vital Statistics in Japan in 2017. Available online: https://www.mhlw.go.jp/ toukei/list/81-1.html (accessed on 7 June 2022). (In Japanese)

5. Wigglesworth, J.S. Experimental growth retardation in the foetal rat. J. Pathol. Bacteriol. 1964, 88, 1–13.

6. Garofano, A.; Czernichow, P.; Breant, B. In utero undernutrition impairs rat beta-cell development. Diabetologia 1997, 40, 1231–1234.

7. Ozaki, T.; Nishina, H.; Hanson, M.A.; Poston, L. Dietary restriction in pregnant rats causes gender-related hypertension and vascular dysfunction in offspring. J. Physiol. 2001, 530, 141–152.

8. Jimenez-Chillaron, J.C.; Hernandez-Valencia, M.; Reamer, C.; Fisher, S.; Joszi, A.; Hirshman, M.; Oge, A.; Walrond, S.; Przybyla, R.; Boozer, C.; et al. β-cell secretory dysfunction in the pathogenesis of low birth weight-associated diabetes: A murine model. Diabetes 2005, 54, 702–711.

9. Simmons, R.A.; Templeton, L.J.; Gertz, S.J. Intrauterine growth retardation leads to the development of type 2 diabetes in the rat. Diabetes 2001, 50, 2279–2286.

10. Ogata, E.S.; Bussey, M.E.; Finley, S. Altered gas exchange, limited glucose and branched chain amino acids, and hypoinsulinism retard fetal growth in the rat. Metabolism 1986, 35, 970–977

11. Nagano N, Kaneko C, Ohashi S, Seya M, Takigawa I, Masunaga K, Morioka I. Non-obese type 2 diabetes with a history of being an extremely preterm small-for-gestational-age infant without early adiposity rebound. Int. J. Environ. Res. Public Health 2022, 19, 8560.

12. Okazaki, M.; Yamashita, S. Recent advances in analytical methods on lipoprotein subclasses: Calculation of particle numbers from lipid levels by gel permeation HPLC using "Spherical Particle Model". J. Oleo Sci. 2016, 65, 265–282.

13. Usui, S.; Hara, Y.; Hosaki, S.; Okazaki, M. A new on-line dual enzymatic method for simultaneous quantification of cholesterol and triglycerides in lipoproteins by HPLC. J. Lipid Res. 2002, 43, 805–814.

14. Okazaki, M.; Usui, S.; Ishigami, M.; Sakai, N.; Nakamura, T.; Matsuzawa, Y.; Yamashita, S. Identification of unique lipoprotein subclasses for visceral obesity by component analysis of cholesterol profile in high-performance liquid chromatography. Arterioscler. Thromb. Vasc. Biol. 2005, 25, 578–584.

15. Ylihärsilä, H.; Kajantie, E.; Osmond, C.; Forsén, T.; Barker, D.J.; Eriksson, J.G. Birth size,

adult body composition and muscle strength in later life. Int. J. Obes. 2007, 31, 1392–1399.

16.   Matinolli, H.M.; Hovi, P.; Männistö, S.; Sipola-Leppänen, M.; Eriksson, J.G.; Mäkitie, O.; Järvenpää, A.L.; Andersson, S.; Kajantie, E. Early protein intake is associated with body composition and resting energy expenditure in young adults born with very low birth weight. J. Nutr. 2015, 145, 2084–2091.

17.   Cho, W.K.; Suh, B.K. Catch-up growth and catch-up fat in children born small for gestational age. Korean J. Pediatr. 2016, 59, 1–7.

18.   Feng, Z.; Hanson, R.W.; Berger, N.A.; Trubitsyn, A. Reprogramming of energy metabolism as a driver of aging. Oncotarget 2016, 7, 15410–15420.

19.   Imai, S.-I.; Guarente, L. NAD+ and sirtuins in aging and disease. Trends Cell Biol. 2014, 24, 464–471.

20.   Granger, D.N.; Kvietys, P.R. Reperfusion injury and reactive oxygen species: The evolution of a concept. Redox Biol. 2015, 6, 524–551.

21.   Crabtree, M.J.; Hale, A.B.; Channon, K.M. Dihydrofolate reductase protects endothelial nitric oxide synthase from uncoupling in tetrahydrobiopterin deficiency. Free Radic. Biol. Med. 2011, 50, 1639–1646.

22.   Rasola, A.; Bernardi, P. The mitochondrial permeability transition pore and its involvement in cell death and in disease pathogenesis. Apoptosis 2007, 12, 815–833.

23.   Yu, N.; Wang, S.; Wang, P.; Li, Y.; Li, S.; Chen, H.; Wang, T. The calcium uniporter regulates the permeability transition pore in isolated cortical mitochondria. Neural Regen. Res. 2012, 7, 109–113.

24.   Sangwung, P.; Petersen, K.F.; Shulman, G.I.; Knowles, J.W. Mitochondrial dysfunction, insulin resistance, and potential genetic implications. Endocrinology 2020, 161, bqaa017.

25.   Wang, X.; Li, H.; Zheng, A.; Yang, L.; Liu, J.; Chen, C.; Tang, Y.; Zou, X.; Li, Y.; Long, J.; et al. Mitochondrial dysfunction-associated OPA1 cleavage contributes to muscle degeneration: Preventative effect of hydroxytyrosol acetate. Cell Death Dis. 2014, 5, e1521.